Characteristics of methanesulfonic acid, non-sea-salt sulfate and organic carbon aerosols over the Amundsen Sea, Antarctica

Jinyoung Jung[1], Sang-Bum Hong[1], Meilian Chen[2,5], Jin Hur[2], Liping Jiao[3], Youngju Lee[1], Keyhong Park[1], Doshik Hahm[4], Jung-Ok Choi[1], Eun Jin Yang[1], Jisoo Park[1], Tae-Wan Kim[1], and SangHoon Lee[1]

[1]Korea Polar Research Institute, 26 Songdomirae-ro, Yeonsu-gu, Incheon 21990, Republic of Korea
[2]Sejong University, 209 Neungdong-ro, Gwangjin-gu, Seoul 05006, Republic of Korea
[3]Third Institute of Oceanography, State Oceanic Administration, Xiamen 361005, China
[4]Pusan National University, Busan 46241, Republic of Korea
[5]Environmental program, Guangdong Technion-Israel Institute of Technology, Shantou 515063, China

Correspondence to: Jinyoung Jung (jinyoungjung@kopri.re.kr)

Abstract. To investigate characteristics of particulate methanesulfonic acid ($MSA_{(p)}$), non-sea-salt sulfate (nss-SO_4^{2-}) and organic carbon (OC) aerosols, aerosol and seawater samples were collected over the Southern Ocean (43°S−70°S) and the Amundsen Sea (70°S−75°S) during the ANA06B cruise conducted in the austral summer of 2016 aboard the Korean icebreaker IBR/V *Araon*. Over the Southern Ocean, atmospheric $MSA_{(p)}$ concentration was low (0.10 ± 0.002 µg m^{-3}), whereas its concentration increased sharply up to 0.57 µg m^{-3} in the Amundsen Sea where *Phaeocystis antarctica* (*P. antarctica*), a producer of dimethylsulfide (DMS), was the dominant phytoplankton species. Unlike $MSA_{(p)}$, mean nss-SO_4^{2-} concentration in the Amundsen Sea was comparable to that in the Southern Ocean. Water-soluble organic carbon (WSOC) concentrations over the Southern Ocean and the Amundsen Sea varied from 0.048–0.16 µgC m^{-3} and 0.070–0.18 µgC m^{-3}, with averages of 0.087 ± 0.038 µgC m^{-3} and 0.097 ± 0.038 µgC m^{-3}, respectively. For water-insoluble organic carbon (WIOC), its mean concentrations over the Southern Ocean and the Amundsen Sea were 0.25 ± 0.13 µgC m^{-3} and 0.26 ± 0.10 µgC m^{-3}, varying from 0.083–0.49 µgC m^{-3} and 0.12–0.38 µgC m^{-3}, respectively. WIOC was the dominant organic carbon species in both the Southern Ocean and the Amundsen Sea, accounting for 73–75% of total aerosol organic carbon. WSOC/Na$^+$ and WIOC/Na$^+$ ratios in the fine mode aerosol particles were higher, especially in the Amundsen Sea where biological productivity was much higher than the Southern Ocean. The fluorescence properties of water-soluble organic aerosols investigated using fluorescence excitation-emission matrix coupled with parallel factor analysis (EEM-PARAFAC) revealed that protein-like components were dominant in our marine aerosol samples, representing 69–91% of the total intensity. Protein-like component also showed a significant positive relationship with the relative biomass of diatoms; however, it was negatively correlated with the relative biomass of *P. antarctica*. These results suggest that protein-like component is most likely produced as a result of biological processes of diatoms in the Amundsen Sea.

1 Introduction

Marine aerosols have been recognized to play an essential role in global climate due to their impact on the radiation budget and cloud microphysics by scattering solar radiation and acting as cloud condensation nuclei (CCN) (Andreae and Crutzen, 1997; O'Dowd et al., 2004). Considerable efforts have been devoted to investigating physicochemical characteristics of marine aerosols to elucidate the source and formation of CCN in the marine environment because of their importance for understanding the cloud-mediated effects of aerosols on climate (e.g., Hegg et al., 1991; O'Dowd et al., 1997; Vallina et al., 2006; Furutani et al., 2008; Meskhidze and Nenes, 2010; Mochida et al., 2011; Gras and Keywood, 2017).

The biogeochemical cycle of sulfur between the marine atmosphere and the ocean has received much attention, especially after the proposal by Charlson et al. (1987) who postulated that the most significant source of CCN in the marine environment is non-sea-salt sulfate (nss-SO_4^{2-}) derived from atmospheric oxidation of dimethylsulfide (DMS). DMS produced by marine phytoplankton is the dominant sulfur species in ocean surface waters and is transported to the atmosphere through sea-to-air flux (Bates et al., 1992). After emission to the atmosphere, DMS is oxidized by the hydroxyl (OH), nitrate (NO_3), and bromine oxide (BrO) radicals to form either gaseous methanesulfonic acid ($MSA_{(g)}$) or sulfur dioxide (SO_2). While $MSA_{(g)}$ rapidly condenses onto existing particles (forming particulate MSA, $MSA_{(p)}$), SO_2 is further oxidized to nss-SO_4^{2-} (e.g., Andreae et al., 1985; Gondwe et al., 2004; Read et al., 2008). The conversion of DMS into nss-SO_4^{2-} aerosols is an essential process because of the potential interaction of sulfur aerosols with incoming solar radiation, and their role on cloud microphysics which could result in a negative climate feedback mechanism (Legrand and Pasteur, 1998). However, Quinn and Bates (2011) questioned the role of sulfur-containing aerosols derived from DMS in the climate feedback, but it is still clear that DMS emission contributes significantly to sulfur-containing aerosols acting as CCN over the oceans (Sanchez et al., 2018).

In addition to atmospheric sulfur species, marine organic aerosols have recently drawn increasing attention due to their potentially significant contribution to CCN budget over the remote ocean (e.g., O'Dowd et al., 2004; Quinn and Bates, 2011; Gantt and Meskhidze, 2013). Ocean surface waters are enriched with small particulate organic materials including phytoplankton, bacteria, viruses, fragments of larger organisms and organic detritus (Quinn and Bates, 2011) as well as dissolved organic matter released or exuded by phytoplankton during growth, predation by grazing organisms and viral lysis (Biersmith and Benner, 1998). The organic fraction in surface waters can be broadly characterized as lipids, amino and fatty acids, mono- and polysaccharides and humic substances (Benner et al., 1992; Mochida et al., 2002; Gantt and Meskhidze, 2013), which can be emitted into the marine atmosphere with sea-salt particles through bubble bursting processes (Russell et al., 2010; Gantt et al., 2011). Previous studies have highlighted the significance of ocean-derived organic aerosol as a critical component of the aerosol-cloud-climate feedback system (e.g., Kawamura et al., 1996; Kanakidou et al., 2005; Kawamura et al., 2010; Russell et al., 2010; Miyazaki et al., 2011; Quinn and Bates, 2011; Fu et al., 2015; Wilson et al., 2015; Miyazaki et al., 2016). For example, O'Dowd et al. (2004) revealed clear differences in ocean-derived organic carbon (OC) concentrations during periods of high and low biological activity, suggesting that OC derived from biological activity can enhance CCN concentration in the marine atmosphere, and that ocean-derived OC is a significant component of the aerosol-cloud-climate feedback system involving marine biota.

Although the importance of marine biogenic source contribution to CCN concentration has motivated numerous studies, quantitative measurements of the size-dependent composition of marine aerosols over high southern latitudes, especially the Antarctic remain sparse, due to its inaccessibility. Because of the difficulty in conducting a field observation, the sources and evolution of aerosols over the Antarctic are still a subject of many open questions (Giordano et al., 2017). It is, therefore, necessary to fill the data gap in the knowledge of marine aerosols in the Antarctic to improve understanding of the effect of ocean ecosystem on the marine aerosol-cloud-climate system.

Polynyas, recurring areas of seasonally open water surrounded by sea ice in high latitude regions, often exhibit high primary productivity (e.g., Arrigo et al., 2003; Arrigo et al., 2012; Yager et al., 2012; Hahm et al., 2014) because they are the first polar marine systems to be exposed to the increasing springtime solar radiation (Arrigo and van Dijken, 2003; Criscitiello et al., 2013). Coastal polynyas surrounding Antarctica exhibit massive phytoplankton blooms during the austral summer (December–February), with most peaking in January. The productive polynyas are located in the Ross and Amundsen Seas while annual production in the polynyas of East Antarctica is generally low (Arrigo and van Dijken, 2003). The Amundsen Sea, located in West Antarctica, hosts two coastal polynyas: the Amundsen Sea Polynya (ASP) and Pine Island Bay Polynya (PIBP) (Arrigo and van Dijken, 2003). The ASP is the most productive polynya (per unit area) among 37 identified coastal polynya systems in the Antarctic (Arrigo and van Dijken, 2003) due to the combined effects of the enhanced light condition (Park et al., 2017), the abundance of macronutrients, supply of iron (Fe) from melting sea ice and/or glaciers and continental shelf sediments resulted from the intrusion of relatively warm, salty, and nutrient-rich Circumpolar Deep Water (CDW) (Arrigo et al., 2012; Dutrieux et al., 2014; Sherrell et al., 2015). Consequently, the Amundsen Sea is an ideal place to monitor a direct link between biological production and local emissions of sulfur compounds and organics, not only because of its remoteness from anthropogenic activity but also because it is an area of exceptionally high seasonal primary production. However, little is known about the distributions of atmospheric sulfur and organic species in the Amundsen Sea.

To understand the influence of marine biological activities on atmospheric marine aerosols in the Amundsen Sea, we have investigated characteristics of $MSA_{(p)}$, nss-SO_4^{2-}, water-soluble organic carbon (WSOC), and water-insoluble organic carbon (WIOC) in marine aerosols collected over the Amundsen Sea, Antarctica. Besides, we have carried out a hydrographic survey to examine the link between biological production and atmospheric sulfur and organic species in the Amundsen Sea. The objectives of this study are to (1) investigate the distributions of $MSA_{(p)}$ and nss-SO_4^{2-} over the Amundsen Sea, (2) examine the factors influencing atmospheric $MSA_{(p)}$ concentration in the Amundsen Sea, (3) investigate the distributions of atmospheric WSOC and WIOC over the Amundsen Sea, and (4) estimate the source of atmospheric water-soluble organic aerosols using a fluorescence technique.

2 Method

Aerosol and seawater samples were collected during the ANA06B cruise conducted over the Southern Ocean and the Amundsen Sea, Antarctica aboard the Korean icebreaker IBR/V *Araon* (Fig. 1). The cruise started from Christchurch, New Zealand on 6 January 2016, sailed over the Amundsen Sea for 23 days (14 January−5 February), and returned to Christchurch, New Zealand on 24 February 2016. In this study, the Southern Ocean and the Amundsen Sea are defined as the regions between

43°S and 70°S, and between 70°S and 75°S, respectively. Although the cruise track covered the Southern Ocean (43°S−70°S) and the Amundsen Sea (70°S−75°S), a significant portion of our cruise was allocated to the ASP and near-ice shelf surveys (< 2 km from ice shelves) adjacent to the Dotson, the Getz, and the Pine Island ice shelves.

2.1 Aerosol collection

Two high-volume aerosol samplers (HV-1000R, Sibata Scientific Technology Ltd.) were installed on the front of the upper deck (20 m a.s.l.) and used to collect marine aerosols on pre-combusted (at 550°C for 6 hours) quartz filters (25 × 20 cm, QR-100, Sibata Scientific Technology Ltd.). Particle size selectors for PM2.5 and PM10 were installed to each aerosol sampler to collect fine (D < 2.5 µm) and coarse modes (2.5 µm < D < 10 µm) aerosols on the filters, respectively. A wind-sector controller was used to avoid contamination from the ship's exhaust during the cruise (Jung et al., 2013, 2014). The wind-sector controller was set to collect marine aerosol samples only when the relative wind directions were within plus or minus 100° relative to the ship's bow and the relative wind speeds were over 1 m s^{-1}. The flow rate was 1000 L min^{-1} and the total sampling time was 3−4 days, representing a total sampling air volume of 1300−4500 m^3. After sampling, the filters were stored frozen at −24°C before chemical analysis. Four procedural blanks were obtained by placing quartz filters in the aerosol sampler for 5 min on idle systems (i.e., no air flow through the filters) and processed as other aerosol samples. Meteorological variables (e.g., wind speed and wind direction) were continuously monitored by weather monitoring systems equipped on the research vessel during the cruise.

2.2 Chemical analysis

2.2.1 Ionic species

The quartz filters, on which aerosols were collected, were cut into four equivalent subsamples. The subsamples were placed in acid-cleaned polypropylene bottles with the dusty side facing up. Fifty ml of Milli-Q water (> 18 MΩ cm^{-1}, Millipore Co.) was added to the bottles, and the bottles were covered using polypropylene screw caps. The subsamples were sonicated for 30 min. The extraction solution was then filtered through a 13-mm diameter, 0.45-µm pore size membrane filter (PTFE syringe filter, Millipore Co.). The filtrates were analyzed by ion chromatography (IC; ICS 2000, Thermo Scientific Dionex) for anions (Cl$^-$, MSA, NO$_3^-$, and SO$_4^{2-}$) and cations (Na$^+$, NH$_4^+$, K$^+$, Mg^{2+}, and Ca^{2+}). The instrumental detection limits were: Cl$^-$ 0.05 µg L^{-1}, MSA 0.02 µg L^{-1}, NO$_3^-$ 0.02 µg L^{-1}, SO$_4^{2-}$ 0.02 µg L^{-1}, Na$^+$ 0.02 µg L^{-1}, NH$_4^+$ 0.14 µg L^{-1}, K$^+$ 0.16 µg L^{-1}, Mg^{2+} 0.08 µg L^{-1}, and Ca^{2+} 0.20 µg L^{-1} (Hong et al., 2015). From replicate injections, the analytical precision was estimated to be < 5%. The concentrations of nss-SO$_4^{2-}$ were calculated as total SO$_4^{2-}$ minus Na$^+$ concentration times 0.2516, the SO$_4^{2-}$/Na$^+$ mass ratio in bulk seawater (Millero and Sohn, 1992).

2.2.2 Water-soluble organic carbon

Other subsamples of the quartz filters were ultrasonically extracted using the same method for ionic species measurements. The filtrates were analyzed by a total organic carbon (TOC) analyzer (Model TOC-L, Shimadzu Inc.) for

determination of total dissolved organic carbon (TDOC), which was defined as water-soluble organic carbon (WSOC) in this study. In the analytical system, inorganic carbon was removed by acidifying the samples to pH 2 by 2 M HCl and sparging for 8 min before analysis of the total carbon content. Carbon dioxide (CO_2) derived from the conversion of TDOC by high temperature (680°C) catalytic oxidation was measured by a nondispersive infrared (NDIR) detector to quantify TDOC (Miyazaki et al., 2011). Milli-Q water and consensus reference material (CRM, 42–45 µM C for DOC, deep Florida Strait water obtained from University of Miami) were measured every sixth analysis to check the accuracy of the measurements. The procedural mean blank for WSOC was 180 µgC L^{-1}, which represented 14% of mean WSOC concentration in aerosols. The detection limit calculated as three times of the standard deviation of the procedural blanks was 21 µgC L^{-1}. The relative standard deviations of WSOC analysis for reproducibility test (at least three measurements per sample) was less than 3%.

2.2.3 Organic and elemental carbon

Concentrations of OC and elemental carbon (EC) were measured using the thermal optical transmission (TOT) method on a Sunset lab OC/EC analyzer (Model-4, USA) (Birch and Cary, 1996). The analytical procedures for OC and EC measurements are described in detail elsewhere (e.g., Miyazaki et al., 2011; Niu et al., 2012, 2013). In brief, a filter punch of 1.54 cm^2 was placed in the oven and heated in a completely pure helium environment up to 850°C to convert all OC into CO_2. For EC measurement, the oven was cooled to 550°C and then heated until the oven temperature stepping up back to 850°C under a 2% oxygen-containing helium environment. All CO_2 derived from the conversion of both OC and EC was measured by an NDIR detector. The equivalent OC concentration from filed blank accounted for ~15% of the average OC concentrations of the actual samples. Based on field blank uncertainties, detection limits for OC and EC were 0.1 µgC cm^{-2} and 0.02 µgC cm^{-2}, respectively. In this study, WIOC was defined as the difference between OC and WSOC (i.e., WIOC = OC − WSOC) (Miyazaki et al., 2011). Using the propagating errors of each parameter, the uncertainty of WIOC concentration was estimated to be 5.8%.

2.2.4 Optical measurements and excitation-emission matrix coupled with parallel factor analysis

Absorption spectra of atmospheric WSOC were obtained from 240 to 800 nm on a Shimadzu 1800 ultraviolet-visible (UV-Vis) spectrophotometer (Shimadzu Inc.). Three-dimensional fluorescence excitation-emission matrices (EEMs) were scanned using a Hitachi F-7000 luminescence spectrometer (Hitachi Inc.) at the excitation/emission (Ex/Em) wavelengths of 250−500/280−550 nm. The excitation and the emission scans were set at 5 nm and 1 nm steps, respectively. The UV–Vis spectra were used for inner filter correction for the EEMs according to McKnight et al. (2001). Further details on the EEM measurements and the procedure of post-acquisition corrections are available in previous studies (Chen et al., 2010, 2017, 2018). The procedure for Raman Unit (RU) normalization can be found elsewhere (Lawaetz and Stedmon, 2009). Parallel factor (PARAFAC) modeling was performed using MATLAB 7.0.4 with the DOMFluor toolbox. All corrected EEMs of aerosol samples were used for modeling. The number of fluorescent components was determined based on split-half validation. The biological index (BIX), an index of recent biological and autochthonous contribution, was calculated according to Huguet et al. (2009).

2.3 Hydrographic data

2.3.1 Chlorophyll-a

2.3.1.1 In situ measurement

Seawater samples were collected from 4 to 5 layers in the upper 100 m at 46 stations in the Amundsen Sea using a conductivity-temperature-depth (CTD) and a rosette system holding 24-10L Niskin bottles (SeaBird Electronics, SBE 911 plus) (Fig. 1). Seawater sample for chlorophyll-a (Chl-a) analysis was filtered through a GF/F filter (47 mm, Whatman), which was then extracted with 90% acetone for 24 hours. Chl-a was measured onboard using a fluorometer (Trilogy, Turner Designs, USA) (Lee et al., 2016).

2.3.1.2 Satellite observation

Monthly composite of sea surface Chl-a concentration (mg m^{-3}) was obtained from Moderate Resolution Imaging Spectroradiometer (MODIS) Aqua data available from the Goddard Space Flight Center, NASA. The spatial resolution of the data was approximately 9 km per pixel (http://oceandata.sci.gsfc.nasa.gov).

2.3.2 Dissolved organic carbon

Seawater sample was drawn from the Niskin bottle by gravity filtration through an inline pre-combusted (at 550°C for 6 hours) Whatman GF/F filter held in an acid-cleaned (0.1 M HCl) polycarbonate 47 mm filter holder (PP-47, ADVANTEC). The filter holder was attached directly to the Niskin bottle spigot. The filtrate was collected in an acid-cleaned glass bottle and then distributed into two pre-combusted 20 ml glass ampoules with a sterilized serological pipette. Each ampoule was sealed with a torch, quick-frozen, and preserved at –24°C until the analysis in our land laboratory. Analysis of dissolved organic carbon (DOC) was performed by high-temperature combustion using a Shimadzu TOC-L analyzer. Milli-Q water (blank) and consensus reference material (CRM, 42–45 µM C for DOC, deep Florida Strait water obtained from University of Miami) were measured every sixth analysis to check the accuracy of the measurements. Analytical errors based on the standard deviations for replicated measurements (at least three measurements per sample) were within 5% for DOC.

2.3.3 Particulate organic carbon

For determination of particulate organic carbon (POC), seawater sample was drawn from the Niskin bottle into an amber polyethylene bottle. Known volumes (500 ml–1 L) of seawater were filtered onto pre-combusted Whatman GF/F filters (25 mm) under gentle vacuum at < 0.1 MPa. The filter samples were stored at –80°C until the analysis in our land laboratory. Before POC analysis, the filter samples were freeze-dried and then exposed to HCl fumes for 24 hours in a desiccator to remove inorganic carbon from the samples. Measurement of POC was carried out with a CHN elemental analyzer (vario MACRO cube, Elementar, Germany). Acetanilide was used as a standard. The precision of these measurements was ± 4%.

2.3.4 Phytoplankton taxonomic composition

Phytoplankton taxonomic composition was assessed using High Performance Liquid Chromatography (HPLC) analysis of accessory photosynthetic pigment concentrations. For the analysis of photosynthetic pigments, 1−2 L of seawater samples were filtered onto 47 mm Whatman GF/F filters and stored at −80°C until the analysis in our land laboratory. The filters were extracted with 3 ml of 100% acetone, ultrasonicated for 30 seconds and maintained under 4°C in dark for 15 hours. Debris was removed by filtering through 0.45 μm Teflon syringe filters. Before injection, the extracts were diluted with distilled water (1 ml of extract plus 0.3 ml of distilled water) to avoid the peak distortion of the first eluting pigments. Pigments were assessed by HPLC analysis following the method of Zapata et al. (2000). Before analysis, the instrument (Agilent series 1200 chromatographic system, Germany) was calibrated using standard pigments (DHI, Denmark). A C_8 column (250 mm × 4.6 mm, 5 μm particle size, Agilent XDB-C8, USA) was used for pigment separation. HPLC pigment data was processed using CHEMTAX (CHEMical TAXonomy), a matrix factorization program to calculate the absolute Chl-a biomass of major algal groups. Twelve pigments were chosen for CHEMTAX analysis, and seven pigment algal groups were defined according to Wright et al. (2010), including *Phaeocystis antarctica* (*P. antarctica*), diatoms, and cryptophytes.

3 Results and discussion

3.1 Atmospheric MSA(p) over the Southern Ocean and the Amundsen Sea

Concentration of MSA(p) in bulk (fine + coarse) aerosols during the cruise ranged from 0.038–0.57 μg m^{-3}, with an average of 0.22 ± 0.14 (mean ± one standard deviation) μg m^{-3}. About ~80% (median values for all data) of MSA(p) existed in the fine mode aerosols. Over the Southern Ocean (43°S−70°S, samples A1–A2), the MSA(p) concentration was relatively low (mean: 0.10 ± 0.002 μg m^{-3}), whereas its concentration over the Amundsen Sea (70°S–75°S, samples A3–A9) increased sharply up to 0.35 μg m^{-3} and showed high spatial variability (range: 0.096–0.57 μg m^{-3}, mean: 0.28 ± 0.15 μg m^{-3}), with the highest value observed in the ASP (Fig. 2a). As expected, however, the MSA(p) concentration gradually decreased from 0.29 μg m^{-3} to 0.038 μg m^{-3} with distance from the ASP (i.e., from the Amundsen Sea to the Southern Ocean, samples, A10–A14, mean: 0.18 ± 0.11 μg m^{-3}). The MSA(p) concentration from this study was in reasonable agreement with previously published results obtained over the regions near the Antarctic continent during the austral summer when air masses originated from the western Antarctic coastal regions (60°S−70°S, 0.05–0.26 μg m^{-3}, Chen et al., 2012). However, our mean MSA(p) concentration in the Amundsen Sea was about 1.8–4.4 times higher than those observed at Antarctic research stations during the austral summer, such as Palmer Station (64.77°S, 64.05°W, 0.122 ± 0.127 μg m^{-3}, December 1990–March 1991, Savoie et al., 1993), Halley Station (75°35′S, 26°19′W, 0.14 μg m^{-3}, January–February 2005, Read et al., 2008), Neumayer Station (70°39′S, 8°15′W, 0.154 ± 0.077 μg m^{-3}, monthly mean in January from 1983–1995, Minikin et al., 1998), and Dumont D'Urville Station (66°40′S, 140°1′E, 0.063 ± 0.019 μg m^{-3}, monthly mean in January from 1991–1995, Minikin et al., 1998). Although the mean MSA(p) concentration was much higher than those observed at the Antarctic research stations, the maximum of MSA(p) in the Amundsen Sea was comparable to the highest concentration measured at Palmer Station (0.57 μg m^{-3}, Savoie et al., 1993), implying that the source strength for MSA(p) is greater in the Amundsen Sea. These differences in atmospheric MSA(p)

concentrations among coastal Antarctic regions presumably reflect regional differences in factors controlling MSA$_{(p)}$ abundance in the marine atmosphere, such as spatial variations of phytoplankton bloom, phytoplankton taxonomic composition, emission flux of DMS, atmospheric oxidative capacity, atmospheric transport and removal (Minikin et al., 1998; Gondwe et al., 2004; Chen et al., 2012; Criscitiello et al., 2013; Jung et al., 2014).

3.2 Factors influencing atmospheric MSA$_{(p)}$ concentration over the Amundsen Sea

Various factors appear to influence atmospheric MSA$_{(p)}$ concentration in the Amundsen Sea. According to Arrigo and van Dijken (2003), 5 years (1997–2002) averaged Chl-a level in the ASP during the month of January (6.98 ± 3.32 mg m^{-3}) is more than 2 times higher than that in the Ross Sea Polynya (2.67 ± 0.82 mg m^{-3}). Indeed, satellite ocean color images (http://oceancolor.sci.gsfc.nasa.gov) exhibited persistently high Chl-a levels in the ASP during the sampling period (Fig. 3), implying a strong influence of biogenic source on atmospheric MSA$_{(p)}$ in the Amundsen Sea.

In addition to the high productivity, phytoplankton taxonomic assemblages could be a significant factor influencing atmospheric MSA$_{(p)}$ abundance. In general, phytoplankton taxonomic abundances in the Amundsen Sea are dominated by haptophyte *P. antarctica* (e.g., Lee et al., 2016; Yager et al., 2016), which produces large amounts of DMS in Antarctic waters (Liss et al., 1994; Schoemann et al., 2005). During the cruise, *P. antarctica* was the dominant phytoplankton species in the upper 50 m, accounting for $42 \pm 19\%$ of phytoplankton biomass (Chl-a), with lesser abundances of diatoms ($39 \pm 17\%$) found throughout the polynya and sea ice zone (see Supplement, Fig. S1). In addition, extremely high concentrations (> 150 nM) and fluxes (85 ± 119 µmol m^{-2} d^{-1}) of DMS have been observed in the region where phytoplankton assemblages were dominated by *P. antarctica* during the cruise (Kim et al., 2017), which are consistent with previous results observed in the Amundsen Sea (Tortell et al., 2012).

We investigated the relationships between atmospheric MSA$_{(p)}$ concentration and the variables mentioned above, to examine factors influencing atmospheric MSA$_{(p)}$ concentration in the Amundsen Sea. Atmospheric MSA$_{(p)}$ concentration showed no relationship with either in situ sea surface Chl-a concentration ($r = 0.029$, $p > 0.05$) (Fig. S2) or the relative biomass of *P. antarctica* ($r = 0.30$, $p > 0.05$). This suggests that Chl-a concentration and phytoplankton taxonomic composition are not direct factors determining atmospheric MSA$_{(p)}$ concentration over the Amundsen Sea.

To investigate the relationship between atmospheric MSA$_{(p)}$ and DMS flux, we used the DMS flux data reported by Kim et al. (2017), who calculated sea–air DMS fluxes using sea surface DMS concentrations and shipboard wind speed data monitored during our cruise. Details of the measurement of sea surface DMS concentration and the sea–air DMS flux calculation are given by Kim et al. (2017). The DMS flux (reported by Kim et al., 2017) averaged for the duration of each aerosol sampling showed a somewhat similar variation trend to that of atmospheric MSA$_{(p)}$ concentration (Fig. 4a), but no correlation was found between atmospheric MSA$_{(p)}$ and DMS flux ($r = 0.18$, $p > 0.05$, Fig. 4b). DMS fluxes typically rely on gas transfer velocity (k), which is frequently parameterized as a function of wind speed (Wanninkhof, 2014). Measurement and parameterization of the gas transfer velocity are more challenging and subject to greater uncertainty, particularly at high wind speeds (Smith et al., 2018). Wanninkhof et al. (2014) reported that there is a considerable uncertainty in k, especially, under the strong wind condition. About 20% uncertainty was estimated at a global mean wind speed (7.3 m s^{-1}). When we

applied four different k values (W92, W99, N00, W14), the uncertainty in DMS flux in the Amundsen Sea region was about 25%. As the gas transfer velocity increases with increasing wind speed, DMS flux can be overestimated especially, in higher latitudes where DMS is commonly found at high concentrations in surface water, and where both low temperatures and high winds are typical (McGillis et al., 2000). In addition to the uncertainty in DMS flux, the insignificant relationship between atmospheric $MSA_{(p)}$ and DMS flux could result from various complexities in the rate of oxidation of DMS to form atmospheric $MSA_{(p)}$ and long-range transport of atmospheric $MSA_{(p)}$ from biogenically active region, given the lifetime of DMS is approximately 1–2 days (Kloster et al., 2006; Read et al., 2008). Although we found no significant relationship between atmospheric $MSA_{(p)}$ concentration, in situ sea surface Chl-a concentration, the relative biomass of *P. antarctica* and the local sea–air DMS flux, the higher atmospheric $MSA_{(p)}$ concentrations observed over the Amundsen Sea compared to those over the Southern Ocean and in coastal Antarctic regions most likely resulted from complex linkage between these factors.

3.3 Atmospheric nss-SO_4^{2-} over the Southern Ocean and the Amundsen Sea

Concentration of nss-SO_4^{2-} in bulk (fine + coarse) aerosols during the cruise ranged from 0.30–0.87 μg m^{-3}, with ~79% (median values for all data) of nss-SO_4^{2-} being present on fine mode aerosols (Fig. 2b). Mean concentration of nss-SO_4^{2-} during the cruise was 0.61 ± 0.17 μg m^{-3}. Over the Southern Ocean (43°S−70°S, samples A1–A2 and A11–A14), the nss-SO_4^{2-} concentration ranged from 0.30–0.87 μg m^{-3} (mean: 0.60 ± 0.23 μg m^{-3}), whereas its concentration over the Amundsen Sea (70°S–75°S, samples A3–A10) varied from 0.49–0.81 μg m^{-3} (mean: 0.62 ± 0.10 μg m^{-3}). Surprisingly, our mean nss-SO_4^{2-} concentration in the Amundsen Sea was about 1.5 and 2.5 times higher than those observed at American Samoa (14.25°S, 170.58°W, 0.41 ± 0.17 μg m^{-3}, seasonal average (December–February) from 1990–1992, Savoie et al., 1994) and over the South Pacific (8°S–55°S, mean: 0.25 ± 0.17 μg m^{-3}, range: 0.094–0.62 μg m^{-3}, January–March 2009, Jung et al., 2014), respectively. In addition, the mean nss-SO_4^{2-} concentration in the Amundsen Sea was also a factor of 1.6–4.4 higher than those observed at Palmer Station (0.24 ± 0.16 μg m^{-3}, December 1990–March 1991, Savoie et al., 1993), Halley Station (0.14 ± 0.017 μg m^{-3}, monthly mean in January from 1991–1993, Legrand and Pasteur, 1998), Neumayer Station (0.38 ± 0.13 μg m^{-3}, monthly mean in January from 1983–1995, Minikin et al., 1998), and Dumont D'Urville Station (0.34 ± 0.039 μg m^{-3}, monthly mean in January from 1991–1995, Minikin et al., 1998) during the austral summer.

Unlike $MSA_{(p)}$, the mean nss-SO_4^{2-} concentration in the Amundsen Sea was comparable to that in the Southern Ocean, although the variation trend of nss-SO_4^{2-} in the Amundsen Sea was similar to that of $MSA_{(p)}$, suggesting that nss-SO_4^{2-} was affected by marine source and large-scale transport (Korhonen et al., 2008). Indeed, nss-SO_4^{2-} showed a strong correlation (r = 0.98, p < 0.01) with $MSA_{(p)}$ in the Amundsen Sea, whereas no relationship was found between them in the Southern Ocean (r = 0.51, p > 0.05) (Fig. S3), suggesting that the local emission of DMS is a significant source of nss-SO_4^{2-} in the Amundsen Sea. It is worth mentioning that nss-SO_4^{2-} can be formed from the homogeneous nucleation of new particles involving H_2SO_4 or from the condensation of gas-phase DMS oxidation products onto existing particles (e.g., Covert et al., 1992; Quinn and Bates, 2011). Recently, Sanchez et al. (2018) identified two types of SO_4^{2-} particles using an Event-Trigger Aerosol-Mass-Spectrometer (ET-AMS), and reported that 63% of SO_4^{2-} was derived from newly formed particles in the free troposphere and 38% of SO_4^{2-} was formed from the condensation of DMS products onto existing particles in the clean marine conditions,

revealing the importance of phytoplankton-produced DMS emission for CCN in the Atlantic. In this study, it is hard to distinguish nss-SO_4^{2-} derived from new particle formation from nss-SO_4^{2-} formed by the condensation of DMS products onto existing particles because of the limitations related to the method to collect data. However, the significant correlation of nss-SO_4^{2-} with $MSA_{(p)}$ in the Amundsen Sea suggests that DMS emission from the Amundsen Sea plays a crucial role in the formation of nss-SO_4^{2-} aerosol particles that can act as CCN.

On the other hand, a possible explanation for the insignificant relationship between nss-SO_4^{2-} and $MSA_{(p)}$ in the Southern Ocean is entrainment of nucleated nss-SO_4^{2-} particles into the marine boundary layer of the Southern Ocean from the free troposphere by turbulent diffusion and large-scale transport (Korhonen et al., 2008; Woodhouse et al., 2010). Sanchez et al. (2018) reported that the lack of correlation between SO_4^{2-} particle and atmospheric DMS (or its oxidation products) could result from the competition for DMS and its oxidation products with the competing sinks of condensation onto existing particles and vertical transport to the free troposphere. The lack of correlation between nss-SO_4^{2-} and $MSA_{(p)}$ in the Southern Ocean, therefore, could have resulted from the input of nss-SO_4^{2-} from the free troposphere. Although our data set is not sufficiently complete to allow a meaningful analysis of this likely explanation, the result for nss-SO_4^{2-} concentrations from this study would be valuable for filling the data gap, especially for the Amundsen Sea during the austral summer, and be helpful for validation of modeling of sulfur-containing aerosols.

3.4 $MSA_{(p)}$/nss-SO_4^{2-} ratios over the Southern Ocean and the Amundsen Sea

There have been several field studies investigating the $MSA_{(p)}$/nss-SO_4^{2-} ratio in the Southern Ocean during the austral summer (range: 0.32–0.53, the South Pacific (40°S−45°S), Berresheim et al., 1990; range: 0.12–0.24, Cape Grim (40°41′S , 144°41′E), Ayers et al., 1991; range: 0.17–0.32, the South Pacific (30°S−60°S), Bates et al., 1992; range: 0.096–0.49, the South Pacific (40°S−56°S), Jung et al., 2014).

During the cruise, the $MSA_{(p)}$/nss-SO_4^{2-} ratio in bulk aerosols varied from 0.12 to 0.70 (mean: 0.35 ± 0.17), with lower ratios in marine aerosols collected over the Southern Ocean (range: 0.12–0.51, mean: 0.26 ± 0.14) and higher values over the Amundsen Sea (range: 0.20–0.70, mean: 0.44 ± 0.16), showing a similar variation trend (r = 0.92, p < 0.01) to that of $MSA_{(p)}$ (Fig. 5). This result suggests that atmospheric $MSA_{(p)}$ plays a key role in the variation in $MSA_{(p)}$/nss-SO_4^{2-} ratio over the Southern Ocean and the Amundsen Sea during the austral summer since atmospheric nss-SO_4^{2-} concentrations in the Southern Ocean were quite comparable to the values in the Amundsen Sea.

3.5 Atmospheric WSOC and WIOC over the Southern Ocean and the Amundsen Sea

Concentration of WSOC in bulk (fine + coarse) aerosols during the cruise ranged from 0.048–0.18 µgC m^{-3}, with an average of 0.092 ± 0.037 µgC m^{-3} (Fig. 6a). The WSOC concentrations over the Southern Ocean (43°S−70°S, samples A1–A2 and A11–A14) and the Amundsen Sea (70°S–75°S, samples A3–A9) varied from 0.048–0.16 µgC m^{-3} and 0.070–0.18 µgC m^{-3}, with averages of 0.087 ± 0.038 µgC m^{-3} and 0.097 ± 0.038 µgC m^{-3}, respectively. For WIOC, its mean concentrations over the Southern Ocean and the Amundsen Sea were 0.25 ± 0.13 µgC m^{-3} and 0.26 ± 0.10 µgC m^{-3}, varying from 0.083–0.49 µgC m^{-3} and 0.12–0.38 µgC m^{-3}, respectively (Fig. 6b). We expected much higher WSOC and WIOC concentrations in the

Amundsen Sea than the Southern Ocean because of extremely high Chl-a concentration in the Amundsen Sea (Fig. 3). However, no significant differences of mean WSOC and WIOC concentrations were found between the Southern Ocean and the Amundsen Sea, suggesting that Chl-a concentration is not a direct factor controlling atmospheric OC concentration in our study area (Quinn et al., 2014), although a significant correlation between atmospheric OC and Chl-a concentrations was observed in the Austral Ocean (Amsterdam Island, 37°48′S, 77°34′E, Sciare et al., 2009).

Both WSOC and WIOC mainly existed in fine mode particles, and the percentages of WSOC and WIOC present in fine aerosol particles were ~93% and ~74%, respectively (median value for all data). During the cruise, WIOC was the dominant OC species in both the Southern Ocean and the Amundsen Sea, accounting for 75% and 73% of total aerosol organic carbon, respectively (Fig. 6c). These results were consistent with the previous studies. For example, O'Dowd et al. (2004) observed a dominant water-insoluble OC fraction (~45%) in fine marine aerosol collected during periods of phytoplankton bloom in the North Atlantic. Moreover, Facchini et al. (2008a) reported that OC observed through a bubble bursting experiment and a field measurement (at Mace Head) was mainly water-insoluble, accounting for 77 ± 5% of the primary marine aerosol fraction in the submicron size range, and that WIOC consisted of colloids and aggregates exuded by phytoplankton. Given that atmospheric WIOC is mechanically produced through bubble bursting processes from hydrophobic organic matter that accumulates in the ocean surface (Facchini et al., 2008a; Gantt et al., 2011; Miyazaki et al., 2011), the dominance of WIOC suggests that water-insoluble organic matter exuded by phytoplankton is more accumulated in sea surface water and emitted into the marine atmosphere via bubble bursting and breaking waves by local wind.

Our mean values of WSOC and WIOC in the Amundsen Sea were comparable to the results by Sciare et al. (2009) who reported that the mean concentrations of WSOC and WIOC observed at Amsterdam Island (37°48′S, 77°34′E) during the austral summer (January) were 0.083 ± 0.028 µgC m^{-3} and 0.19 ± 0.062 µgC m^{-3}, respectively. It is worth noting that atmospheric WSOC and WIOC show seasonal variations, with maximum values during austral summer (January) and minimum concentrations during winter (Sciare et al., 2009). These variations are attributable to pronounced seasonal variations in biogenic marine productivity. Given that our study was carried out during the austral summer, the concentrations of WIOC and WSOC from this study would be considered as maximum values in the Amundsen Sea. Although our results were supported by previous studies as mentioned above, the spatial variability in WSOC and WIOC concentrations has been observed over various oceanic regions by previous studies. For instance, Fu et al. (2015) reported that atmospheric OC species concentrations observed at Alert, in the Canadian High Arctic were 0.186 µgC m^{-3} (range: 0.041–0.30 µgC m^{-3}) for WSOC and 0.068 µgC m^{-3} (range: 0.022–0.12 µgC m^{-3}) for WIOC. The results by Fu et al. (2015) were 1.9 times higher and 3.8 times lower than our mean concentrations of WSOC and WIOC in the Amundsen Sea, respectively. In addition, Miyazaki et al. (2011) reported that mean concentrations of WSOC and WIOC observed over the western North Pacific (40°N–44°N) were 0.65 ± 0.27 µgC m^{-3} and 0.56 ± 0.19 µgC m^{-3}, which were a factor of 6.7 and 2.2 higher than those in the Amundsen Sea, respectively. These differences in WSOC and WIOC concentrations among the oceanic regions presumably reflect regional differences in factors influencing atmospheric WSOC and WIOC concentrations, such as source strength for volatile organic compounds emitted from biogenic sources (BVOCs), atmospheric oxidative capacity (e.g., OH, NO$_3$ and ozone),

meteorological condition (e.g., wind speed), DOC and POC concentrations in sea surface water, atmospheric transport and removal (e.g., Facchini et al., 1999; Kanakidou et al., 2005; Sun et al., 2006).

3.6 WIOC/Na$^+$ and WSOC/Na$^+$ ratios and relationships of WIOC and WSOC with Na$^+$ over the Southern Ocean and the Amundsen Sea

5   Breaking waves on the ocean surface generate air bubbles that scavenge organic matter from seawater. When injected into the atmosphere, these bubbles burst, yielding sea spray aerosols enriched in organic matter, relative to seawater (Quinn et al., 2014). Sea spray aerosols have been defined as the hydrated droplets encapsulating dissolved sea-salt and entrained organic matter (O'Dowd et al., 2008). Previous studies have revealed that organic matter is enriched in sea spray aerosol particles produced by bubble bursting processes in the fine and ultrafine aerosol size fractions, suggesting that sea spray aerosol particles

10 have an important role in transferring organic matter from the sea surface to the atmosphere (Facchini et al., 2008a; O'Dowd et al., 2008). During the cruise, ~76% of Na$^+$, a tracer of sea spray, was associated with the coarse mode particle (Fig. 7a). Moreover, statistically significant relationships were found between mean wind speed and Na$^+$ concentrations in fine (r = 0.54, p < 0.05) and coarse (r = 0.69, p < 0.01) mode aerosols, reflecting that Na$^+$ was formed from bubble bursting by local wind. Although Na$^+$ was predominantly associated with the coarse mode particle, WSOC/Na$^+$ and WIOC/Na$^+$ in the fine mode

15 aerosol particles were higher than those in the coarse mode aerosol particles, especially in the Amundsen Sea where biological productivity was much higher than the Southern Ocean (Fig. 7b). In the Southern Ocean, the WSOC/Na$^+$ ratio in the fine mode particles varied from 0.045–0.40, whereas the WSOC/Na$^+$ ratio in the Amundsen Sea ranged from 0.17–0.89. The average WSOC/Na$^+$ ratio in the Amundsen Sea (0.40 ± 0.24) was substantially higher than that in the Southern Ocean (0.16 ± 0.12). For the WIOC/Na$^+$ ratio in the fine mode particles, similar results were observed. The WIOC/Na$^+$ ratios in the Southern Ocean

20 and the Amundsen Sea varied from 0.038–0.97 and 0.26–2.4, with averages of 0.35 ± 0.31 and 0.91 ± 0.73, respectively; however, WIOC/Na$^+$ ratio in the fine mode aerosol particles was much higher than WSOC/Na$^+$, suggesting that bubble bursting at the ocean surface is a major source of atmospheric WIOC and that WIOC is more accumulated in the sea surface water. These results show that the higher marine biological activities in the Amundsen Sea can be a significant factor leading to the higher OC/Na$^+$ ratios, indicating a linkage between OC emission and biological activities (Fig. 3).

25   Because sea spray aerosols are emitted as a result of wind-driven bubble bursting, correlations of organic aerosol mass concentrations with sea spray aerosols (i.e., Na$^+$), whose concentration are related to local wind speeds, have been used to attribute their origin to marine sources because submicron Na$^+$ is known to form primary aerosols from evaporating seawater droplets (Russell et al., 2010). In this study, we investigated relationships of WIOC and WSOC concentrations with Na$^+$ concentration in the fine modes since both WIOC and WSOC were primarily associated with the fine mode particles (Figs. 6a

30 and 6b). The submicron WIOC showed no statistically significant relationships with submicron Na$^+$ over the Southern Ocean and the Amundsen Sea (Fig. 8a), although WIOC/Na$^+$ ratio in the fine mode aerosol particles was much higher (Fig. 7b). Similarly, Boreddy et al. (2018) found no correlation between sea-salt and WIOC in the western North Pacific. The increase in sea-salt particle flux under higher wind speed conditions shifts the sea spray aerosol size distribution towards larger sizes and accelerates their dry deposition and gravitational settling from the atmosphere (de Leeuw et al., 2011). Thus, theses

insignificant relationships between WIOC and Na^+ in the fine modes could result from the differences in local wind speeds and local biological activities, because wind speed, a key factor determining sea spray aerosols, controls the local flux rather than local concentration of marine particles (Monahan and O'Muircheartaigh, 1986). Our results are further supported by the study of Ceburnis et al. (2008), who found WIOC and sea-salt exhibited upward fluxes observed through gradient flux measurements, suggesting a primary production mechanism for WIOC. Although we found no significant relationships between WIOC and Na^+ in the fine modes, the high WIOC/Na^+ ratio in the fine mode aerosol particles (Fig. 7b) indicates that WIOC was predominantly of primary origin (Ceburnis et al., 2008). However, the WIOC production by secondary processes cannot be completely excluded either (Ceburnis et al., 2016), but we have no evidence of that.

Unlike the relationship between WIOC and Na^+, submicron WSOC showed a strong correlation ($r = 0.94$, $p < 0.01$) with submicron Na^+ in the Amundsen Sea (Fig. 8b). In addition, we also found a significant correlation ($r = 0.93$, $p < 0.01$) between WSOC and MSA$_{(p)}$ concentrations in the Amundsen Sea (Fig. 8c). However, in the Southern Ocean, WSOC showed no significant relationship with submicron Na^+ or MSA$_{(p)}$. MSA$_{(p)}$ is produced by atmospheric oxidation of DMS, which is released as a gas phase from marine biological activities and thus can be used as an indicator of secondary aerosols of marine biogenic origin (Miyazaki et al., 2011). Consequently, the strong correlations between WSOC, Na^+ and MSA$_{(p)}$ in the Amundsen Sea implies that the Amundsen Sea that has the most productive polynya in the Antarctic is a strong source region of BVOCs, and that WSOC was formed by the condensation of BVOCs released from sea surface onto preexisting submicron sea spray aerosols through gas-to-particle conversion due to a higher surface-to-volume ratio of submicron aerosols (Romakkaniemi et al., 2011). On the other hand, the poor correlations between WSOC, Na^+, and MSA$_{(p)}$ in the Southern Ocean implies the differences in local source strength of BVOCs and that the presence of DMS in seawater and its subsequent oxidation to MSA$_{(p)}$ were not necessarily linked to the formation of submicron WSOC over the Southern Ocean (Miyazaki et al., 2016).

3.7 Fluorescence properties of water-soluble organic aerosols over the Southern Ocean and the Amundsen Sea

Fluorescence excitation-emission matrix coupled with parallel factor analysis (EEM-PARAFAC) has been widely used to investigate the sources and optical properties of dissolved organic matter in terrestrial and oceanic systems (e.g., Coble, 1996, 2007; Stedmon et al., 2003; Yamashita et al., 2011; Retelletti Brogi et al., 2018). Moreover, recent field studies demonstrated that EEM-PARAFAC provides useful information for characterizing atmospheric OC in aerosols and rainwater (e.g., Fu et al., 2015; Miyazaki et al., 2018; Yang et al., 2019).

As described in section 3.6, our results strongly suggested that the submicron WSOC observed in the Amundsen Sea was formed by the condensation of BVOCs onto preexisting submicron sea spray aerosols by showing the strong correlations with Na^+ and MSA$_{(p)}$. To further elucidate the sources of water-soluble organic aerosols, we investigated the fluorescence properties of submicron aerosols using EEM-PARAFAC. Fluorophores in water-soluble organic aerosols were divided into three primary types on the basis of their peak position (Fig. 9). The spectral features of component 1 (C1, Ex/Em: 300/344 nm) was similar to the component previously identified in in coastal and oceanic waters as well as the polar ocean and was thought to be phytoplankton-derived (or ice algae-derived) protein-like component (Stedmon et al., 2007, 2011, Retelletti Brogi et al.,

2018). Component 2 (C2, Ex/Em: 276/326 nm) was assigned as a tryptophan-like fluorophore, which has been considered to be a labile component produced as a result of biological production in marine environments (Coble et al., 1998; Yamashita and Tanoue 2003). Component 3 (C3, Ex/Em: <260/458 nm) spectra were characterized as representing terrestrial humic-like fluorophores (Coble et al., 1996; Yamashita and Tanoue, 2003; Chen et al., 2010; Chen et al., 2018). During the cruise, the C1 fluorescence intensity was much higher and variable, varying between 0.0133 and 0.139 RU (Fig. 10a). In comparison, the fluorescence intensity of C2 (range: 0.0195–0.0518 RU) and C3 (range: 0.00857–0.0351 RU) was much less variable. Among the three components, the protein-like C1 was the dominant fluorescence component in our marine aerosol samples, accounting for 31–73% of the total intensity, and the relative contributions of tryptophan-like C2 and terrestrial humic-like C3 were found to represent 17–50% and 8–31%, respectively (Fig. 10b). In our marine aerosol samples, protein-like components (i.e., C1 and C2) represented 69–91% of the total intensity.

Despite the extremely high Chl-a concentration in the Amundsen Sea (Fig. 3), we found no significant difference of the average values of protein-like C1 and tryptophan-like C2 fluorescence intensity between the Amundsen Sea and the Southern Ocean. However, relatively much higher values of C1 and C2 fluorescence intensity were observed when the ship approached the Amundsen Sea (i.e., samples A3 and A4), passing through the sea ice zone (Figs. 1b and 10a). The C1 and C2 fluorescence intensity values sharply decreased and remained relatively low in the Amundsen Sea, and then gradually increased from the Amundsen Sea to the Southern Ocean. As mentioned in section 3.2, *P. antarctica* was the dominant phytoplankton species in the Amundsen Sea, whereas diatoms formed a major group in the marginal sea ice zone (Lee et al., 2016).

Ice algae, commonly found in polar sea ice and surrounding waters, are largely dominated by diatoms (Roberts et al., 2007), which are an important contributor to aerosols by emission of aerosol-forming volatile (e.g., alkyl-amines) and non-volatile (e.g., mycosporine-like amino acids) organic nitrogen in the Antarctic sea ice region (Dall'Osto et al., 2017). Previous studies (e.g., Facchini et al., 2008b; Miyazaki et al., 2011) provided the evidence that volatile emissions of alkyl-amine from marine algae can represent an important source of marine secondary organic aerosol. Moreover, Dall'Osto et al. (2017) observed that the fluorescence signal for protein-like component was positively correlated to organic nitrogen originated from the melted Antarctic sea ice floes, indicating that protein-like component was associated with organic nitrogen derived from the microbiota of sea ice and sea ice-influenced ocean. Although we have no aerosol water-soluble organic nitrogen dataset, our results provide additional evidence that marine algae can influence fluorescent property of marine aerosols. Interestingly, we found that fluorescence intensity of C1 showed a significant positive relationship with the relative biomass of diatoms (r = 0.89, p < 0.01); however, it was negatively correlated with the relative biomass of *P. antarctica* (r = –0.79, p < 0.05) (Figs. 10c and 10d). Given the dominance of diatoms in the marginal sea ice zone during the cruise and the significant positive relationship between fluorescence intensity of protein-like C1 and the relative biomass of diatoms, it is plausible, therefore, that biological processes of diatoms are an important factor in controlling the abundance of protein-like component in water-soluble organic aerosols over the Southern Ocean and the Amundsen Sea, although further studies are necessary to clarify this point.

The biological index (BIX) has been used to estimate the contribution of autochthonous biological activity (Fu et al., 2015; Miyazaki et al., 2018). An increase in BIX is related to an increase in the contribution of microbially derived organics.

High BIX values (> 1) have been shown to correspond to a predominantly biological or microbial origin of dissolved organic matter and to the presence of organic matter freshly released into water, whereas low values (< 0.6) indicate little biological material (Huguet et al., 2009). In this study, the BIX values ranged from 1.17–3.61, with an average of 2.23 ± 0.807 (Fig. 10b). The high BIX values also supported that the fluorescence properties of WSOC were influenced by marine biological activities.

4 Conclusions

Characteristics of atmospheric sulfur (i.e., $MSA_{(p)}$ and nss-SO_4^{2-}) and OC (i.e., WSOC and WIOC) species in marine aerosols, and the environmental factors influencing their distributions were investigated over the Southern Ocean and the Amundsen Sea during the austral summer. In the Amundsen Sea, atmospheric $MSA_{(p)}$ concentration drastically increased (up to 0.57 µg m^{-3}), suggesting significant influences of marine biological activities on atmospheric $MSA_{(p)}$. The higher $MSA_{(p)}$ concentration was attributed to exceptionally high seasonal primary production during the austral summer, the dominance of *P. antarctica* with respect to phytoplankton biomass, and extremely high DMS concentrations produced by DMS-producing algae species (e.g., *P. antarctica*) in the Amundsen Sea.

WIOC was the dominant OC species in both the Southern Ocean and the Amundsen Sea, accounting for 75% and 73%, respectively. Despite extremely high Chl-a concentration in the Amundsen Sea, no significant differences of mean WSOC and WIOC concentrations were found between the Southern Ocean and the Amundsen Sea. However, the higher WSOC/Na$^+$ and WIOC/Na$^+$ ratios were observed in the submicron aerosol particles, especially in the Amundsen Sea where biological productivity was much higher than the Southern Ocean.

It is worth noting that the simultaneous measurements of chemical species in marine aerosols as well as chemical and biological properties of seawater in the Amundsen Sea allowed a better understanding of the effect of ocean ecosystem on OC species. Moreover, the fluorescence properties of water-soluble organic aerosols revealed that protein-like components are most likely produced as a result of biological processes of diatoms.

West Antarctica is one of the fastest-warming regions globally (Bromwich et al., 2013). Ice shelves and glaciers in the Amundsen Sea have been shrinking at a remarkable rate (Rignot et al., 2008). Moreover, sea ice coverage is decreasing fast in the western Antarctic (Stammerjohn et al., 2012). Because ocean buoyancy, stratification, and trace metal distribution are affected by these changes, the regional oceanography, phytoplankton community structure and biogeochemical cycles of sulfur and carbon in the Amundsen Sea are likely affected as well (Yager et al., 2012). Further studies, therefore, are required to understand more clearly biogeochemical cycles of sulfur and carbon between the ocean and the marine atmosphere and should focus on long-term monitoring of atmospheric sulfur and OC species in the Amundsen Sea.

5 Data availability

The data used in this study is available on request to the correspondence author Jinyoung Jung (jinyoungjung@kopri.re.kr).

Author contributions

JJ designed the research, carried out the experiments, processed the data, and wrote the paper. SBH, MC and LJ analyzed the aerosol samples. YL and EJY provided the marine biological data. JOC and JP helped in obtaining satellite products. JH, KP, DH and EJY contributed the scientific discussion and paper correction. TWK and SHL organized the field campaign.

Acknowledgements

We are grateful to the captain and crews of IBR/V *Araon* for their enthusiastic assistance during the ANA06B cruise. This study was supported by grants from Korea Polar Research Institute (KOPRI) (PE20160 and PE20140).

References

10 Andreae, M. O. and Crutzen, P. J.: Atmospheric Aerosols: Biogeochemical Sources and Role in Atmospheric Chemistry, Science, 276(5315), 1052–1058, doi:10.1126/science.276.5315.1052, 1997.

Andreae, M. O., Ferek, R. J., Bermond, F., Byrd, K. P., Engstrom, R. T., Hardin, S., Houmere, P. D., LeMarrec, F., Raemdonck, H. and Chatfield, R. B.: Dimethyl sulfide in the marine atmosphere, J. Geophys. Res., 90(D7), 12891–12900, doi:10.1029/JD090iD07p12891, 1985.

15 Arrigo, K. R., Lowry, K. E. and van Dijken, G. L.: Annual changes in sea ice and phytoplankton in polynyas of the Amundsen Sea, Antarctica, Deep-Sea Res. Pt. II, 71-76(c), 5–15, doi:10.1016/j.dsr2.2012.03.006, 2012.

Arrigo, K. R. and van Dijken, G. L.: Phytoplankton dynamics within 37 Antarctic coastal polynya systems, J. Geophys. Res., 108(C8), 3271, doi:10.1029/2002JC001739, 2003.

Arrigo, K. R., Worthen, D. L. and Robinson, D. H.: A coupled ocean-ecosystem model of the Ross Sea: 2. Iron regulation of

20 phytoplankton taxonomic variability and primary production, J. Geophys. Res., 108(C7), 3231, doi:10.1029/2001JC000856, 2003.

Ayers, G. P., Ivey, J. P. and Gillett, R. W.: Coherence between seasonal cycles of dimethyl sulphide, methanesulphonate and sulphate in marine air, Nature, 349(6308), 404–406, doi:10.1038/349404a0, 1991.

Bates, T. S., Calhoun, J. A. and Quinn, P. K.: Variations in the methanesulfonate to sulfate molar ratio in submicrometer

25 marine aerosol particles over the South Pacific Ocean, J. Geophys. Res. Atmos., 97(D9), 9859–9865, doi:10.1029/92JD00411, 1992.

Benner, R., Pakulski, J. D., McCarthy, M., Hedges, J. I. and Hatcher, P. G.: Bulk chemical characteristics of dissolved organic matter in the ocean, Science, 255(5051), 1561–1564, doi:10.1126/science.255.5051.1561, 1992.

Berresheim, H., Andreae, M. O., Ayers, G. P., Gillett, R. W., Merrill, J. T., Davis, V. J. and Chameides, W. L.: Airborne

30 measurements of dimethylsulfide, sulfur dioxide, and aerosol ions over the Southern Ocean South of Australia, J. Atmos. Chem., 10(3), 341–370, doi:10.1007/BF00053868, 1990.

Biersmith, A. and Benner, R.: Carbohydrates in phytoplankton and freshly produced dissolved organic matter, Mar. Chem., 63(1-2), 131–144, doi:10.1016/S0304-4203(98)00057-7, 1998.

Birch, M. E. And Cary, R. A.: Elemental carbon-based method for monitoring occupational exposures to particulate diesel exhaust, Aerosol. Sci. Technol., 25, 221–241, 1996.

5   Boreddy, S. K. R., Haque, M. M. and Kawamura, K.: Long-term (2001–2012) trends of carbonaceous aerosols from a remote island in the western North Pacific: an outflow region of Asian pollutants, Atmos. Chem. Phys., 18(2), 1291–1306, doi:10.5194/acp-18-1291-2018, 2018.

Bromwich, D. H., Nicolas, J. P., Monaghan, A. J., Lazzara, M. A., Keller, L. M., Weidner, G. A. and Wilson, A. B.: Central West Antarctica among the most rapidly warming regions on Earth, Nature Geosci, 6(2), 1–8, doi:10.1038/ngeo1671,
10   2013.

Ceburnis, D., O'Dowd, C. D., Jennings, G. S., Facchini, M. C., Emblico, L., Decesari, S., Fuzzi, S. and Sakalys, J.: Marine aerosol chemistry gradients: Elucidating primary and secondary processes and fluxes, Geophys. Res. Lett., 35(7), L07804, doi:10.1029/2008GL033462, 2008.

Ceburnis, D., Rinaldi, M., Ovadnevaite, J., Martucci, G., Giulianelli, L. and O'Dowd, C. D.: Marine submicron aerosol
15   gradients, sources and sinks, Atmos. Chem. Phys., 16(19), 12425–12439, doi:10.5194/acp-16-12425-2016, 2016.

Charlson, R. J., Lovelock, J. E., Andreae, M. O. and Warren, S. G.: Oceanic phytoplankton, atmospheric sulfur, cloud albedo and climate, Nature, 326(6114), 655–661, doi:10.1038/326655a0, 1987.

Chen, L., Wang, J., Gao, Y., Xu, G., Yang, X., Lin, Q. and Zhang, Y.: Latitudinal distributions of atmospheric MSA and MSA/nss-SO_4^{2-} ratios in summer over the high latitude regions of the Southern and Northern Hemispheres, J. Geophys.
20   Res., 117(D10), D10306, doi:10.1029/2011JD016559, 2012.

Chen, M., Price, R. M., Yamashita, Y. and Jaffé, R.: Comparative study of dissolved organic matter from groundwater and surface water in the Florida coastal Everglades using multi-dimensional spectrofluorometry combined with multivariate statistics, Appl. Geochem., 25(6), 872–880, doi:10.1016/j.apgeochem.2010.03.005, 2010.

Chen, M., Jung, J., Lee, Y. K. and Hur, J.: Surface accumulation of low molecular weight dissolved organic matter in surface
25   waters and horizontal off-shelf spreading of nutrients and humic-like fluorescence in the Chukchi Sea of the Arctic Ocean, Sci. Total Environ., 639, 624–632, doi:10.1016/j.scitotenv.2018.05.205, 2018.

Chen, M., Kim, J.-H., Choi, J., Lee, Y. K. and Hur, J.: Biological early diagenesis and insolation-paced paleoproductivity signified in deep core sediment organic matter, Sci. Rep., 1–11, doi:10.1038/s41598-017-01759-4, 2017.

Coble, P. G.: Characterization of marine and terrestrial DOM in seawater using excitation-emission matrix spectroscopy, Mar.
30   Chem., 51(4), 325–346, doi:10.1016/0304-4203(95)00062-3, 1996.

Coble, P. G.: Marine optical biogeochemistry: The chemistry of ocean color, Chem. Rev., 107(2), 402–418, doi:10.1021/cr050350+, 2007.

Coble, P. G., Del Castillo, C. E. and Avril, B.: Distribution and optical properties of CDOM in the Arabian Sea during the 1995 Southwest Monsoon, Deep-Sea Res. Pt. II, 45(10-11), 2195–2223, doi:10.1016/S0967-0645(98)00068-X, 1998.

Covert, D. S., Kapustin, V. N., Quinn, P. K. and Bates, T. S.: New particle formation in the marine boundary layer, J. Geophys. Res., 97(D18), 20581–20589, 1992.

Criscitiello, A. S., Das, S. B., Evans, M. J., Frey, K. E., Conway, H., Joughin, I., Medley, B. and Steig, E. J.: Ice sheet record of recent sea-ice behavior and polynya variability in the Amundsen Sea, West Antarctica, J. Geophys. Res. Oceans, 118(1), 118–130, doi:10.1029/2012JC008077, 2013.

Dall'Osto, M., Ovadnevaite, J., Paglione, M., Beddows, D. C. S., Ceburnis, D., Cree, C., Cortes, P., Zamanillo, M., Nunes, S. O., Perez, G. L., Ortega-Retuerta, E., Emelianov, M., Vaque, D., Marrase, C., Estrada, M., Sala, M. M., Vidal, M., Fitzsimons, M. F., Beale, R., Airs, R., Rinaldi, M., Decesari, S., Facchini, M. C., Harrison, R. M., O'Dowd, C. and Simo, R.: Antarctic sea ice region as a source of biogenic organic nitrogen in aerosols, Sci Rep, 7(1), 1–10, doi:10.1038/s41598-017-06188-x, 2017.

de Leeuw, G., Andreas, E. L., Anguelova, M. D., Fairall, C. W., Lewis, E. R., O'Dowd, C., Schulz, M. and Schwartz, S. E.: Production flux of sea spray aerosol, Rev. Geophys., 49(2), doi:10.1029/2010RG000349, 2011.

Dutrieux, P., De Rydt, J., Jenkins, A., Holland, P. R., Ha, H. K., Lee, S. H., Steig, E. J., Ding, Q., Abrahamsen, E. P. and Schröder, M.: Strong sensitivity of Pine Island ice-shelf melting to climatic variability, Science, 343(6167), 174–178, doi:10.1126/science.1244341, 2014.

Fu, P., Kawamura, K., Chen, J., Qin, M., Ren, L., Sun, Y., Wang, Z., Barrie, L. A., Tachibana, E., Ding, A. and Yamashita, Y.: Fluorescent water-soluble organic aerosols in the High Arctic atmosphere, Sci. Rep., 5(1), 1053–8, doi:10.1038/srep09845, 2015.

Furutani, H., Dall'osto, M., Roberts, G. C. and Prather, K.: Assessment of the relative importance of atmospheric aging on CCN activity derived from field observations, Atmos. Environ., 42(13), 3130–3142, doi:10.1016/j.atmosenv.2007.09.024, 2008.

Facchini, M. C., Mircea, M., Fuzzi, S., Charlson, R.: Cloud albedo enhancement by surface-active organic solutes in growing droplets, Nature, 401, 257–259, 1999.

Facchini, M. C., Rinaldi, M., Decesari, S., Carbone, C., Finessi, E., Mircea, M., Fuzzi, S., Ceburnis, D., Flanagan, R., Nilsson, E. D., de Leeuw, G., Martino, M., Woeltjen, J. and O'Dowd, C. D.: Primary submicron marine aerosol dominated by insoluble organic colloids and aggregates, Geophys. Res. Lett., 35(17), 396, doi:10.1029/2008GL034210, 2008a.

Facchini, M. C., Decesari, S., Rinaldi, M., Carbone, C., Finessi, E., Mircea, M., Fuzzi, S., Moretti, F., Tagliavini, E., Ceburnis, D. and O'Dowd, C. D.: Important source of marine secondary organic aerosol from biogenic amines, Environ. Sci. Technol., 42(24), 9116–9121, doi:10.1021/es8018385, 2008b.

Gantt, B. and Meskhidze, N.: The physical and chemical characteristics of marine primary organic aerosol: a review, Atmos. Chem. Phys., 13(8), 3979–3996, doi:10.5194/acp-13-3979-2013, 2013.

Gantt, B., Meskhidze, N., Facchini, M. C., Rinaldi, M., Ceburnis, D. and O'Dowd, C. D.: Wind speed dependent size-resolved parameterization for the organic mass fraction of sea spray aerosol, Atmos. Chem. Phys., 11(16), 8777–8790, doi:10.5194/acp-11-8777-2011, 2011.

Giordano, M. R., Kalnajs, L. E., Avery, A., Goetz, J. D., Davis, S. M. and DeCarlo, P. F.: A missing source of aerosols in Antarctica – beyond long-range transport, phytoplankton, and photochemistry, Atmos. Chem. Phys., 17(1), 1–20, doi:10.5194/acp-17-1-2017, 2017.

Gondwe, M., Krol, M., Klaassen, W., Gieskes, W. and de Baar, H.: Comparison of modeled versus measured MSA:nss $SO_4^=$ ratios: A global analysis, Global Biogeochem. Cy., 18(2), GB2006, doi:10.1029/2003GB002144, 2004.

Gras, J. L. and Keywood, M.: Cloud condensation nuclei over the Southern Ocean: wind dependence and seasonal cycles, Atmos. Chem. Phys., 17(7), 4419–4432, doi:10.5194/acp-17-4419-2017, 2017.

Hahm, D., Rhee, T. S., Kim, H.-C., Park, J., Kim, Y. N., Shin, H. C. and Lee, S.: Spatial and temporal variation of net community production and its regulating factors in the Amundsen Sea, Antarctica, J. Geophys. Res. Oceans, 119(5), 2815–2826, doi:10.1002/2013JC009762, 2014.

Hegg, D. A., Ferek, R. J., Hobbs, P. V. and Radke, L. F.: Dimethyl sulfide and cloud condensation nucleus correlations in the Northeast Pacific Ocean, J. Geophys. Res. Atmos., 96(D7), 13189–13191, doi:10.1029/91JD01309, 1991.

Hong, S. -B., Lee, K., Hur, S. -D., Hong, S., Soyol-Erdene, T. -O., Kim, S. -M., Chung, J. -W., Jun, S. -J. and Kang, C. -H.: Development of Melting System for Measurement of Trace Elements and Ions in Ice Core, Bull. Korean Chem. Soc., 36(4), 1069–1081, doi:10.1002/bkcs.10198, 2015.

Huguet, A., Vacher, L., Relexans, S., Saubusse, S., Froidefond, J. M. and Parlanti, E.: Properties of fluorescent dissolved organic matter in the Gironde Estuary, Org. Geochem., 40(6), 706–719, doi:10.1016/j.orggeochem.2009.03.002, 2009.

Jung, J., Furutani, H., Uematsu, M., Kim, S. and Yoon, S.: Atmospheric inorganic nitrogen input via dry, wet, and sea fog deposition to the subarctic western North Pacific Ocean, Atmos. Chem. Phys., 13(1), 411–428, doi:10.5194/acp-13-411-2013, 2013.

Jung, J., Furutani, H., Uematsu, M. and Park, J.: Distributions of atmospheric non-sea-salt sulfate and methanesulfonic acid over the Pacific Ocean between 48°N and 55°S during summer, Atmos. Environ., 99(C), 374–384, doi:10.1016/j.atmosenv.2014.10.009, 2014.

Kanakidou, M., Seinfeld, J. H., Pandis, S. N., Barnes, I., Dentener, F. J., Facchini, M. C., Van Dingenen, R., Ervens, B., Nenes, A., Nielsen, C. J., Swietlicki, E., Putaud, J. P., Balkanski, Y., Fuzzi, S., Horth, J., Moortgat, G. K., Winterhalter, R., Myhre, C., Tsigaridis, K., Vignati, E., Stephanou, E. G. and Wilson, J.: Organic aerosol and global climate modelling: a review, Atmos. Chem. Phys., 5(4), 1053–1123, 2005.

Kawamura, K., Kasukabe, H. and Barrie, L. A.: Secondary formation of water-soluble organic acids and α-dicarbonyls and their contributions to total carbon and water-soluble organic carbon: Photochemical aging of organic aerosols in the Arctic spring, J. Geophys. Res., 115, D21306, doi:10.1029/2010JD014299, 2010.

Kawamura, K., Seméré, R., Imai, Y., Fujii, Y. and Hayashi, M.: Water soluble dicarboxylic acids and related compounds in Antarctic aerosols, J. Geophys. Res., 101(D13), 18721–18728, doi:10.1029/96JD01541, 1996.

Kim, I., Hahm, D., Park, K., Lee, Y., Choi, J. -O., Zhang, M., Chen, L., Kim, H. -C. and Lee, S.: Characteristics of the horizontal and vertical distributions of dimethyl sulfide throughout the Amundsen Sea Polynya, Sci. Total Environ., 584-585(C), 154–163, doi:10.1016/j.scitotenv.2017.01.165, 2017.

Kloster, S., Feichter, J., Maier-Reimer, E., Six, K. D., Stier, P. and Wetzel, P.: DMS cycle in the marine ocean-atmosphere system – a global model study, Biogeosci., 3(1), 29–51, doi:10.5194/bg-3-29-2006, 2006.

Korhonen, H., Carslaw, K. S., Spracklen, D. V., Mann, G. W. and Woodhouse, M. T.: Influence of oceanic dimethyl sulfide emissions on cloud condensation nuclei concentrations and seasonality over the remote Southern Hemisphere oceans: A global model study, J. Geophys. Res., 113(15), D15204, doi:10.1029/2007JD009718, 2008.

Lawaetz, A. J., and Stedmon, C. A.: Fluorescence Intensity Calibration Using the Raman Scatter Peak of Water, Appl. Spectrosc., 63(8), 936–940, doi:10.1366/000370209788964548, 2009.

Lee, Y., Yang, E. J., Park, J., Jung, J., Kim, T. W. and Lee, S.: Physical-biological coupling in the Amundsen Sea, Antarctica: Influence of physical factors on phytoplankton community structure and biomass, Deep-Sea Res. Pt. I, 117(C), 51–60, doi:10.1016/j.dsr.2016.10.001, 2016.

Legrand, M., and Pasteur, E. C.: Methane sulfonic acid to non-sea-salt sulfate ratio in coastal Antarctic aerosol and surface snow, J. Geophys. Res., 103(D9), 10991–11006, 1998.

Liss, P. S., Malin, G., Turner, S. M. and Holligan, P. M.: Dimethyl sulphide and *Phaeocystics*: A review, J. Mar. Syst., 5, 41–53, 1994.

McKnight, D. M., Boyer, E. W., Westerhoff, P. K., Doran, P. T., Kulbe, T. and Andersen, D. T.: Spectrofluorometric characterization of dissolved organic matter for indication of precursor organic material and aromaticity, Limnol. Oceanogr., 46(1), 38–48, doi:10.4319/lo.2001.46.1.0038, 2001.

McGillis, W. R., Dacey, J., Frew, N. M., Bock, E. J. and Nelson, R. K.: Water-air flux of dimethylsulfide, J. Geophys. Res. Oceans, 105(C1), 1187–1193, doi:10.1029/1999JC900243, 2000.

Meskhidze, N. and Nenes, A.: Effects of ocean ecosystem on marine aerosol-cloud interaction, Adv. Meteorol., 2010(4923), 1–13, doi:10.1155/2010/239808, 2010.

Millero, F. J. and Sohn, M. L.: Chemical Oceanography, CRC Press, Boca Raton, FL, 521 pp., 1992.

Minikin, A., Legrand, M., Hall, J., Wagenbach, D., Kleefeld, C., Wolff, E., Pasteur, E. C. and Ducroz, F.: Sulfur-containing species (sulfate and methanesulfonate) in coastal Antarctic aerosol and precipitation, J. Geophys. Res., 103(D9), 10975–10990, doi:10.1029/98JD00249, 1998.

Miyazaki, Y., Coburn, S., Ono, K., Ho, D. T., Pierce, R. B., Kawamura, K. and Volkamer, R.: Contribution of dissolved organic matter to submicron water-soluble organic aerosols in the marine boundary layer over the eastern equatorial Pacific, Atmos. Chem. Phys., 16(12), 7695–7707, doi:10.5194/acp-16-7695-2016, 2016.

Miyazaki, Y., Kawamura, K., Jung, J., Furutani, H. and Uematsu, M.: Latitudinal distributions of organic nitrogen and organic carbon in marine aerosols over the western North Pacific, Atmos. Chem. Phys., 11(7), 3037–3049, doi:10.5194/acp-11-3037-2011, 2011.

Miyazaki, Y., Yamashita, Y., Kawana, K., Tachibana, E., Kagami, S., Mochida, M., Suzuki, K. and Nishioka, J.: Chemical transfer of dissolved organic matter from surface seawater to sea spray water-soluble organic aerosol in the marine atmosphere, Sci. Rep., 8(1), 2593, doi:10.1038/s41598-018-32864-7, 2018.

Mochida, M., Kitamori, Y., Kawamura, K., Nojiri, Y. and Suzuki, K.: Fatty acids in the marine atmosphere: Factors governing their concentrations and evaluation of organic films on sea-salt particles, J. Geophys. Res. Atmos., 107(D17), AAC 1–10, doi:10.1029/2001JD001278, 2002.

Mochida, M., Nishita-Hara, C., Furutani, H., Miyazaki, Y., Jung, J., Kawamura, K. and Uematsu, M.: Hygroscopicity and cloud condensation nucleus activity of marine aerosol particles over the western North Pacific, J. Geophys. Res., 116(D6), 6920–16, doi:10.1029/2010JD014759, 2011.

Monahan, E. C. and O'Muircheartaigh, I. G.: Whitecaps and the Passive Remote-Sensing of the Ocean Surface, Int. J. Remote Sens., 7(5), 627–642, doi:10.1080/01431168608954716, 1986.

Niu, Z., Zhang, F., Chen, J., Yin, L., Wang, Sen and Xu, L.: Carbonaceous species in PM2.5 in the coastal urban agglomeration in the Western Taiwan Strait Region, China, Atmos. Res., 122(C), 102–110, doi:10.1016/j.atmosres.2012.11.002, 2013.

Niu, Z., Zhang, F., Kong, X., Chen, J., Yin, L. and Xu, L.: One-year measurement of organic and elemental carbon in size-segregated atmospheric aerosol at a coastal and suburban site in Southeast China, J. Environ. Monit., 14(11), 2961–7, doi:10.1039/c2em30337j, 2012.

O'Dowd, C. D., Facchini, M. C., Cavalli, F., Ceburnis, D., Mircea, M., Decesari, S., Fuzzi, S., Yoon, Y.-J. and Putaud, J.-P.: Biogenically driven organic contribution to marine aerosol, Nature, 431(7009), 676–680, doi:10.1038/nature02959, 2004.

O'Dowd, C. D., Langmann, B., Varghese, S., Scannell, C., Ceburnis, D. and Facchini, M. C.: A combined organic-inorganic sea-spray source function, Geophys. Res. Lett., 35(1), doi:10.1029/2007GL030331, 2008.

O'Dowd, C. D., Lowe, J. A., Smith, M. H., Davison, B., Hewitt, N. and Harrison, R. M.: Biogenic sulphur emissions and inferred non-sea-salt-sulphate cloud condensation nuclei in and around Antarctica, J. Geophys. Res. Atmos., 102(11D), 12839–12854, 1997.

Park, J., Kuzminov, F. I., Bailleul, B., Yang, E. J., Lee, S., Falkowski, P. G. and Gorbunov, M. Y.: Light availability rather than Fe controls the magnitude of massive phytoplankton bloom in the Amundsen Sea polynyas, Antarctica, Limnol. Oceanogr., 62(5), 2260–2276, doi:10.1002/lno.10565, 2017.

Quinn, P. K. and Bates, T. S.: The case against climate regulation via oceanic phytoplankton sulphur emissions, Nature, 480(7375), 51–56, doi:10.1038/nature10580, 2011.

Quinn, P. K., Bates, T. S., Schulz, K. S., Coffman, D. J., Frossard, A. A., Russell, L. M., Keene, W. C. and Kieber, D. J.: Contribution of sea surface carbon pool to organic matter enrichment in sea spray aerosol, Nature Geosci., 7(3), 228–232, doi:10.1038/NGEO2092, 2014.

Read, K. A., Lewis, A. C., Bauguitte, S., Rankin, A. M., Salmon, R. A., Wolff, E. W., Saiz-Lopez, A., Bloss, W. J., Heard, D. E., Lee, J. D. and Plane, J. M. C.: DMS and MSA measurements in the Antarctic Boundary Layer: impact of BrO on MSA production, Atmos. Chem. Phys., 8, 2985–2997, 2008.

Retelletti Brogi, S., Ha, S.-Y., Kim, K., Derrien, M., Lee, Y. K. and Hur, J.: Optical and molecular characterization of dissolved organic matter (DOM) in the Arctic ice core and the underlying seawater (Cambridge Bay, Canada): Implication for increased autochthonous DOM during ice melting, Sci. Total Environ., 627, 802–811, doi:10.1016/j.scitotenv.2018.01.251, 2018.

Rignot, E., Bamber, J. L., van den Broeke, M. R., Davis, C., Li, Y., van de Berg, W. J. and van Meijgaard, E.: Recent Antarctic ice mass loss from radar interferometry and regional climate modelling, Nature Geosci., 1(2), 106–110, doi:10.1038/ngeo102, 2008.

Roberts, D., Craven, M., Cai, M., Allison, I. and Nash, G.: Protists in the marine ice of the Amery Ice Shelf, East Antarctica, Polar Biol., 30, 143–153, 2007.

Romakkaniemi, S., Kokkola, H., Smith, J. N., Prisle, N. L., Schwier, A. N., McNeill, V. F. and Laaksonen, A.: Partitioning of semivolatile surface-active compounds between bulk, surface and gas phase, Geophys. Res. Lett., 38(3), L03807, doi:10.1029/2010GL046147, 2011.

Russell, L. M., Hawkins, L. N., Frossard, A. A., Quinn, P. K. and Bates, T. S.: Carbohydrate-like composition of submicron atmospheric particles and their production from ocean bubble bursting, Proc. Natl. Acad. Sci. USA, 107(15), 6652–6657, doi:10.1073/pnas.0908905107, 2010.

Sanchez, K. J., Chen, C.-L., Russell, L. M., Betha, R., Liu, J., Price, D. J., Massoli, P., Ziemba, L. D., Crosbie, E. C., Moore, R. H., Mueller, M., Schiller, S. A., Wisthaler, A., Lee, A. K. Y., Quinn, P. K., Bates, T. S., Porter, J., Bell, T. G., Saltzman, E. S., Vaillancourt, R. D. and Behrenfeld, M. J.: Substantial seasonal contribution of observed biogenic sulfate particles to cloud condensation nuclei, Sci. Rep., 8(1), doi:10.1038/s41598-018-21590-9, 2018.

Savoie, D. L., Prospero, J. M., Larsen, R. J., Huang, F., Izaguirre, M. A., Huang, R., Snowdon, T. H., Custals, L. and Sanderson C. G.: Nitrogen and sulfur species in Antarctic aerosols at Mawson, Palmer Station, and Marsh (King George Island), J. Atmos. Chem., 17, 95–122, 1993.

Savoie, D. L., Prospero, J. M., Arimoto, R. and Duce, R. A.: Non-sea-salt sulfate and methanesulfonate at American Samoa, J. Geophys. Res., 99(D2), 3587–3596, doi:10.1029/93JD03337, 1994.

Sciare, J., Favez, O., Sarda-Estève, R., Oikonomou, K., Cachier, H. and Kazan, V.: Long-term observations of carbonaceous aerosols in the Austral Ocean atmosphere: Evidence of a biogenic marine organic source, J. Geophys. Res., 114(D15), 1253, doi:10.1029/2009JD011998, 2009.

Schoemann, V., Becquevort, S., Stefels, J., Rousseau, V. and Lancelot, C.: *Phaeocystis* blooms in the global ocean and their controlling mechanisms: a review, J. Sea Res., 53(1-2), 43–66, doi:10.1016/j.seares.2004.01.008, 2005.

Sherrell, R. M., Lagerström, M. E., Forsch, K. O., Stammerjohn, S. E. and Yager, P. L.: Dynamics of dissolved iron and other bioactive trace metals (Mn, Ni, Cu, Zn) in the Amundsen Sea Polynya, Antarctica, Elem. Sci. Anth., 3, 000071–27, doi:10.12952/journal.elementa.000071, 2015.

Smith, M. J., Walker, C. F., Bell, T. G., Harvey, M. J., Saltzman, E. S. and Law, C. S.: Gradient flux measurements of sea-air DMS transfer during the Surface Ocean Aerosol Production (SOAP) experiment, Atmos. Chem. Phys., 18(8), 5861–5877, doi:10.5194/acp-18-5861-2018, 2018.

Spreen, G., Kaleschke, L. and Heygster, G.: Sea ice remote sensing using AMSR-E 89-GHz channels, J. Geophys. Res., 113(C2), C02S03, doi:10.1029/2005JC003384, 2008.

Stammerjohn, S., Massom, R., Rind, D. and Martinson, D.: Regions of rapid sea ice change: An inter-hemispheric seasonal comparison, Geophys. Res. Lett., 39(6), L06501, doi:10.1029/2012GL050874, 2012.

Stedmon, C. A., Markager, S. and Bro, R.: Tracing dissolved organic matter in aquatic environments using a new approach to fluorescence spectroscopy, Mar. Chem., 82(3-4), 239–254, doi:10.1016/S0304-4203(03)00072-0, 2003.

Stedmon, C. A., Thomas, D. N., Granskog, M., Kaartokallio, H., Papadimitriou, S. and Kuosa, H.: Characteristics of dissolved organic matter in Baltic coastal sea ice: Allochthonous or autochthonous origins? Environ. Sci. Technol., 41(21), 7273–7279, doi:10.1021/es071210f, 2007.

Stedmon, C. A., Thomas, D. N., Papadimitriou, S., Granskog, M. A. and Dieckmann, G. S.: Using fluorescence to characterize dissolved organic matter in Antarctic sea ice brines, J. Geophys. Res., 116, G03027, doi:10.1029/2011JG001716, 2011.

Sun, J. M. and Ariya, P. A.: Atmospheric organic and bio-aerosols as cloud condensation nuclei (CCN): A review, Atmos. Environ., 40(5), 795–820, doi:10.1016/j.atmosenv.2005.05.052, 2006.

Tortell, P. D., Long, M. C., Payne, C. D., Alderkamp, A.-C., Dutrieux, P. and Arrigo, K. R.: Spatial distribution of pCO_2, $\Delta O_2/Ar$ and dimethylsulfide (DMS) in polynya waters and the sea ice zone of the Amundsen Sea, Antarctica, Deep-Sea Res. Pt. II, 71-76(c), 77–93, doi:10.1016/j.dsr2.2012.03.010, 2012.

Vallina, S. M., Simó, R. and Gassó, S.: What controls CCN seasonality in the Southern Ocean? A statistical analysis based on satellite-derived chlorophyll and CCN and model-estimated OH radical and rainfall, Global Biogeochem. Cy., 20(1), GB1014, doi:10.1029/2005GB002597, 2006.

Wanninkhof, R.: Relationship between wind speed and gas exchange over the ocean revisited, Limnol. Oceanogr. Methods, 12, 351–362, doi:10.4319/lom.2014.12.351, 2014.

Wilson, T. W., Ladino, L. A., Alpert, P. A., Breckels, M. N., Brooks, I. M., Browse, J., Burrows, S. M., Carslaw, K. S., Huffman, J. A., Judd, C., Kilthau, W. P., Mason, R. H., McFiggans, G., Miller, L. A., Nájera, J. J., Polishchuk, E., Rae, S., Schiller, C. L., Si, M., Temprado, J. V., Whale, T. F., Wong, J. P. S., Wurl, O., Yakobi-Hancock, J. D., Abbatt, J. P. D., Aller, J. Y., Bertram, A. K., Knopf, D. A. and Murray, B. J.: A marine biogenic source of atmospheric ice-nucleating particles, Nature, 525(7568), 234–238, doi:10.1038/nature14986, 2015.

Woodhouse, M. T., Carslaw, K. S., Mann, G. W., Vallina, S. M., Vogt, M., Halloran, P. R. and Boucher, O.: Low sensitivity of cloud condensation nuclei to changes in the sea-air flux of dimethyl-sulphide, Atmos. Chem. Phys., 10(16), 7545–7559, doi:10.5194/acp-10-7545-2010, 2010.

Wright, S. W., van den Enden, R. L., Pearce, I., Davidson, A. T., Scott, F. J. and Westwood, K. J.: Phytoplankton community structure and stocks in the Southern Ocean (30–80º E) determined by CHEMTAX analysis of HPLC pigment signatures, Deep-Sea Res. Pt. II, 57(9-10), 758–778, doi:10.1016/j.dsr2.2009.06.015, 2010.

Yager, P., Sherrell, R., Stammerjohn, S., Alderkamp, A.-C., Schofield, O., Abrahamsen, P., Arrigo, K., Bertilsson, S., Garay, L., Guerrero, R., Lowry, K., Moksnes, P.-O., Ndungo, K., Post, A., Randall-Goodwin, E., Riemann, L., Severmann, S., Thatje, S., van Dijken, G. and Wilson, S.: ASPIRE: The Amundsen Sea Polynya International Research Expedition, Oceanog., 25(3), 40–53, doi:10.5670/oceanog.2012.73, 2012.

Yager, P. L., Sherrell, R. M., Stammerjohn, S. E., Ducklow, H. W., Schofield, O., Ingall, E. D., Wilson, S. E., Lowry, K. E., Williams, C. M., Riemann, L., Bertilsson, S., Alderkamp, A. C., Dinasquet, J., Logares, R., Richert, I., Sipler, R. E., Melara, A. J., Mu, L., Newstead, R. G., Post, A. F., Swalethorp, R. and van Dijken, G. L.: A carbon budget for the

Amundsen Sea Polynya, Antarctica: Estimating net community production and export in a highly productive polar ecosystem, Elem. Sci. Anth., 4, 000140–36, doi:10.12952/journal.elementa.000140, 2016.

Yamashita, Y., Panton, A., Mahaffey, C. and Jaffé, R.: Assessing the spatial and temporal variability of dissolved organic matter in Liverpool Bay using excitation–emission matrix fluorescence and parallel factor analysis, Ocean Dyn., 61(5), 569–579, doi:10.1007/s10236-010-0365-4, 2011.

Yamashita, Y. and Tanoue, E.: Chemical characterization of protein-like fluorophores in DOM in relation to aromatic amino acids, Mar. Chem., 82(3-4), 255–271, doi:10.1016/S0304-4203(03)00073-2, 2003.

Yang, L., Chen, W., Zhuang, W.-E., Cheng, Q., Li, W., Wang, H., Guo, W., Chen, C.-T. A. and Liu, M.: Characterization and bioavailability of rainwater dissolved organic matter at the southeast coast of China using absorption spectroscopy and fluorescence EEM-PARAFAC, Estuarine Coastal Shelf Sci., 217, 45–55, doi:10.1016/j.ecss.2018.11.002, 2019.

Zapata, M., Rodríguez, F. and Garrido, J. L.: Separation of chlorophylls and carotenoids from marine phytoplankton: a new HPLC method using a reversed phase C_8 column and pyridine-containing mobile phases, Mar. Ecol. Prog. Ser., 195, 29–45, doi:10.3354/meps195029, 2000.
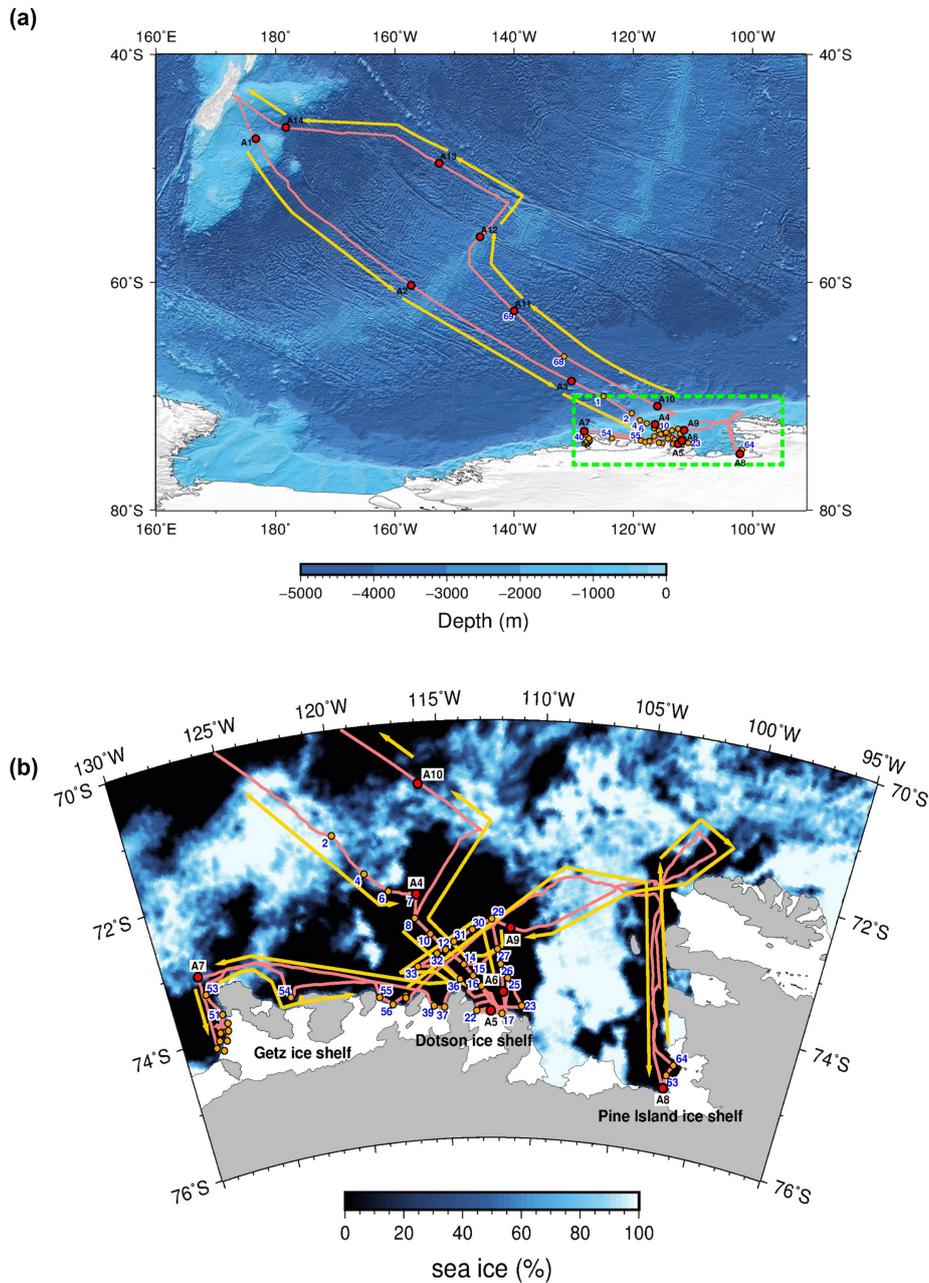
Figure 1: Cruise track of the ANA06B. Panel (a) shows the entire cruise track (pink line) with bathymetry, aerosol (red circles) and seawater sampling (orange circles) locations. Each aerosol sampling start point represents the end of the previous sampling period. Dotted pink line (from Christchurch, New Zealand to A1 sampling location) indicates that no aerosol sampling was conducted. Yellow arrows and green dotted rectangle indicate the moving direction of the ship and the location of the Amundsen Sea, respectively. Panel (b) shows the cruise tack in the Amundsen Sea with sea ice concentration on 6 January 2016. Sea ice concentration was obtained from the Advanced Microwave Scanning Radiometer (AMSR) 2 sea ice maps (Spreen et al., 2008).
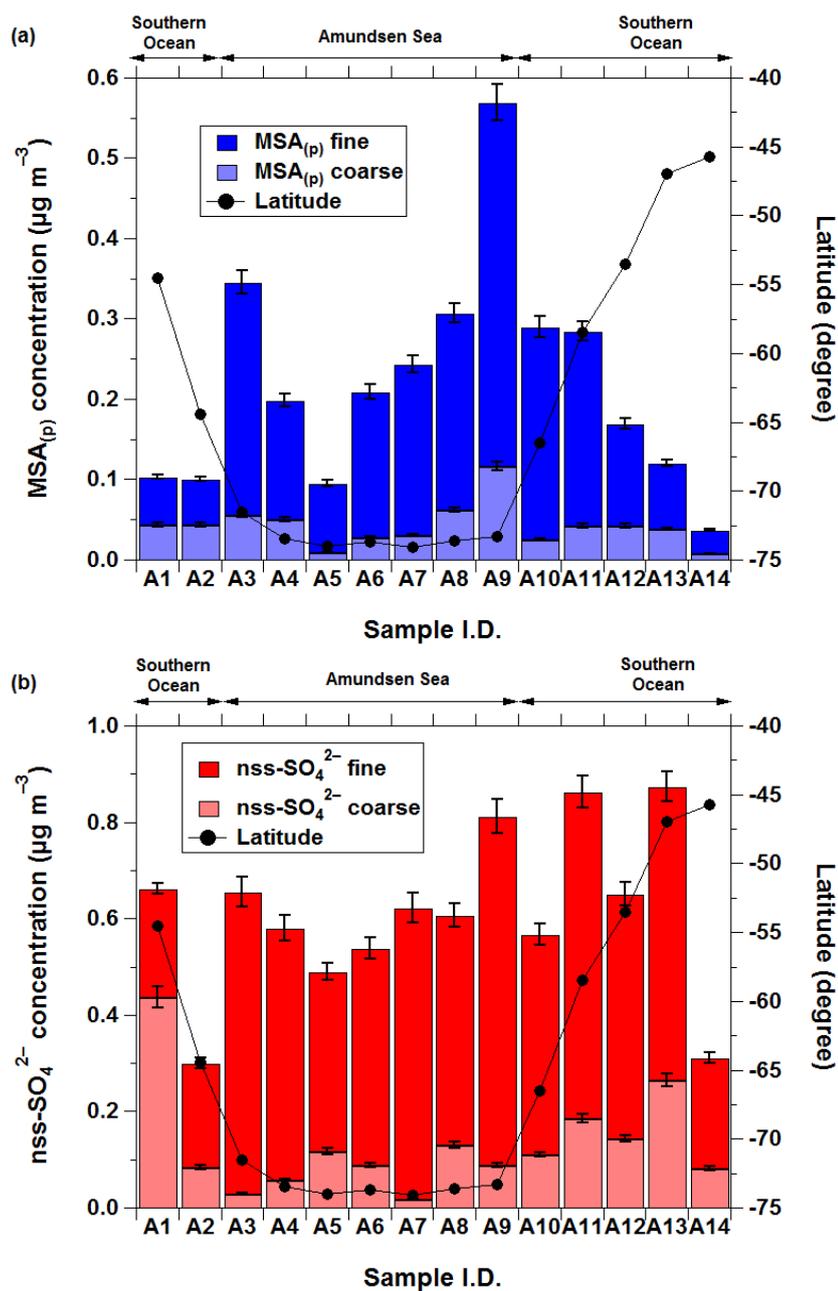
Figure 2. Concentrations of particulate methanesulfonic acid (MSA$_{(p)}$) (a) and non-sea-salt sulfate (nss-SO$_4^{2-}$) (b) against sample I.D. in aerosols collected over the Southern Ocean (43°S−70°S) and the Amundsen Sea (70°S−75°S). Black solid circle lines in panels (a) and (b) indicate the latitude of half-way point between each aerosol sampling start and endpoint. Double arrows in upper panels show the sampling locations of aerosol samples.
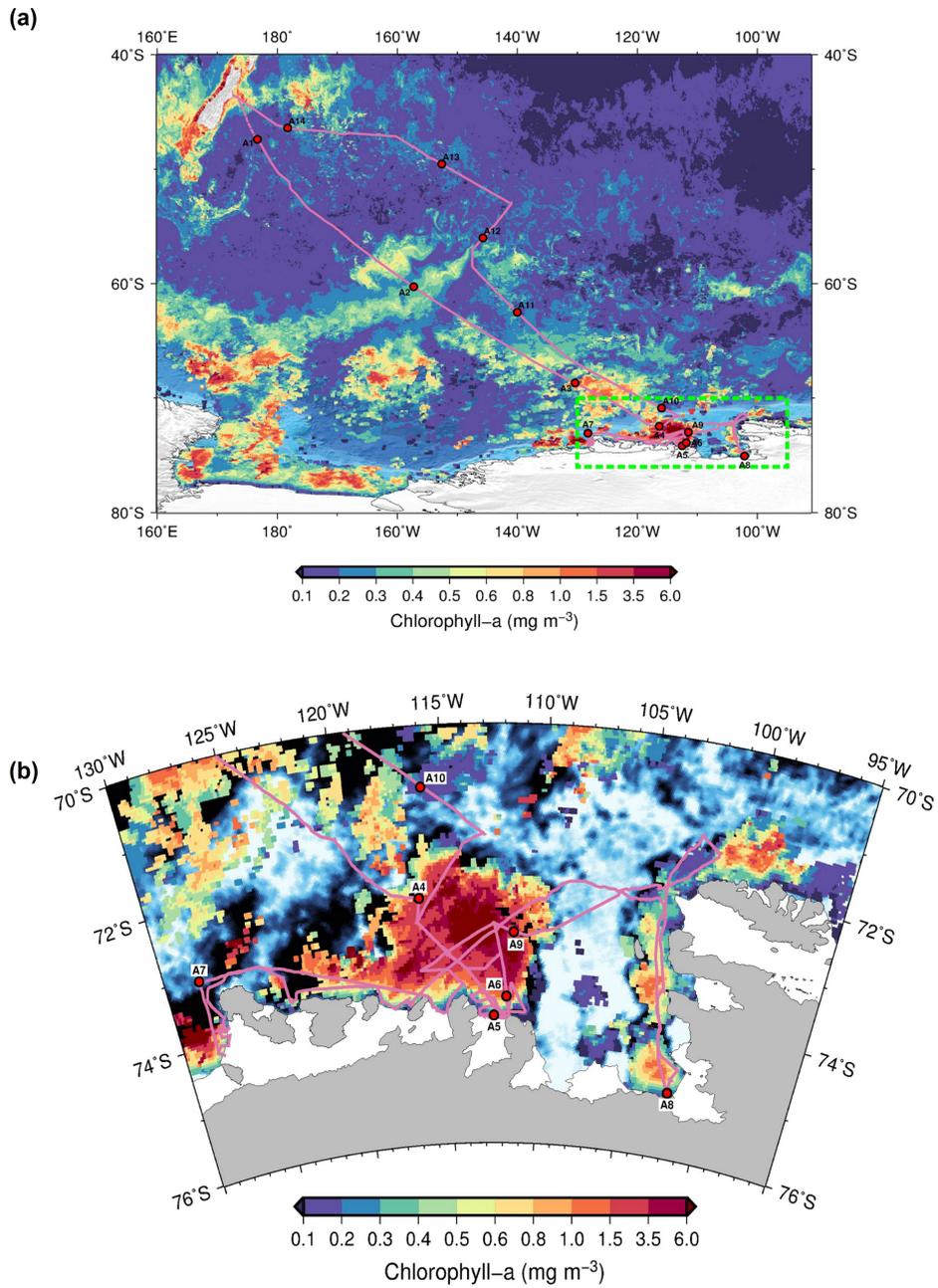
Figure 3. Monthly composite chlorophyll-a concentrations in the Southern Ocean (a) and the Amundsen Sea (b) for January 2016. The cruise track (pink line) and aerosol sampling locations (red circles) are also shown. Each aerosol sampling start point represents the end of the previous sampling period. The green dotted rectangle in panel (a) indicates the location of the Amundsen Sea. Sea ice distribution on 6 January 2016 is shown in panel (b).
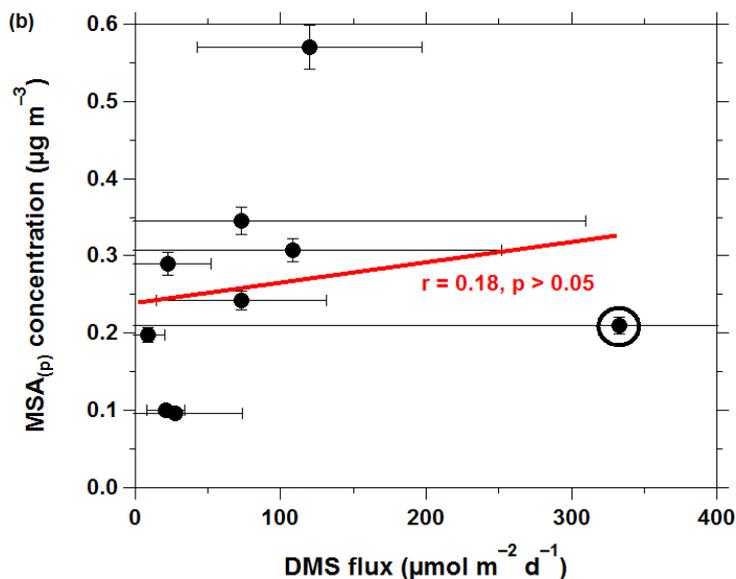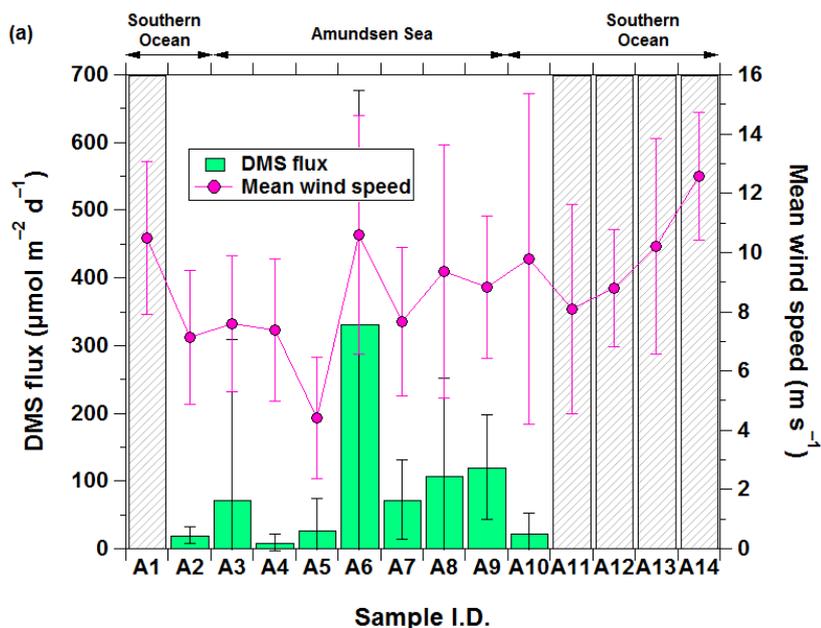
Figure 4. Dimethylsulfide (DMS) flux (reported by Kim et al., 2017) (a) against aerosol sample I.D. and the correlation between MSA$_{(p)}$ concentration and DMS flux (b). The DMS fluxes were calculated using sea surface DMS concentrations and shipboard wind speed data monitored during the cruise. Details of the measurement of sea surface DMS concentration and DMS flux calculation are given by Kim et al. (2017). Each DMS flux in both panels (a) and (b) represents its mean value and standard deviation for each aerosol sampling time. The gray hatched areas in panel (a) denote that no DMS measurement was conducted. Pink solid circle line in panel (a) indicates the mean and standard deviation of wind speeds for each aerosol sampling time. Double arrows in panel (a) show the sampling locations of aerosol samples. In panel (b), the red line indicates the correlation between MSA$_{(p)}$ concentration and DMS flux.
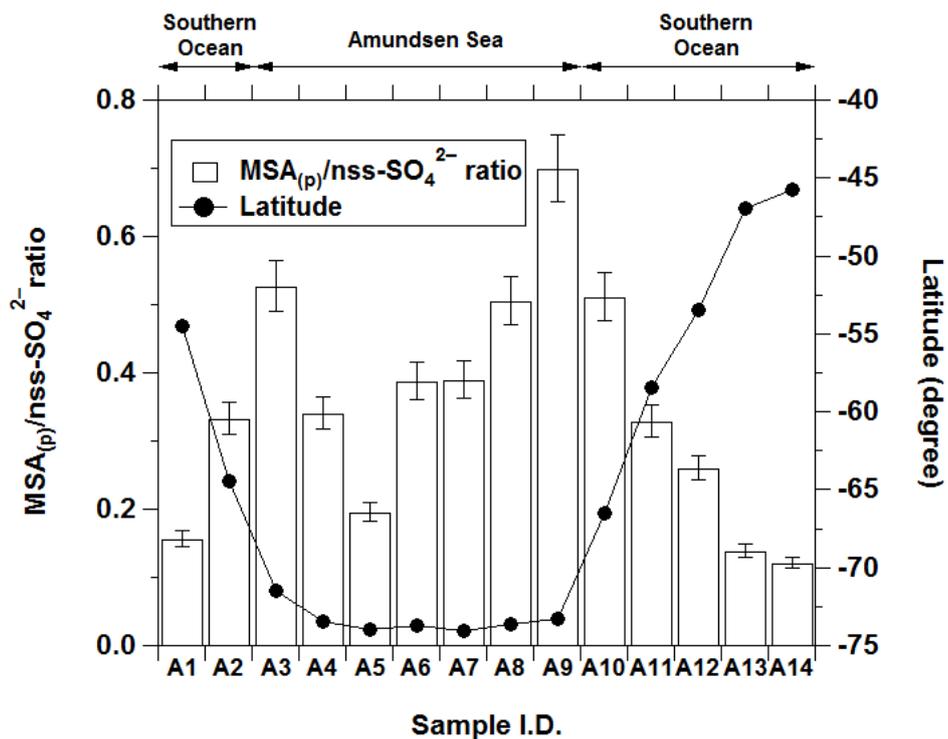
Figure 5. MSA(p)/nss-SO4²⁻ ratio against aerosol sample I.D. Double arrows in upper panel show the sampling locations of aerosol samples. Black solid circle lines indicate the latitude of half-way point between each aerosol sampling start and endpoint.
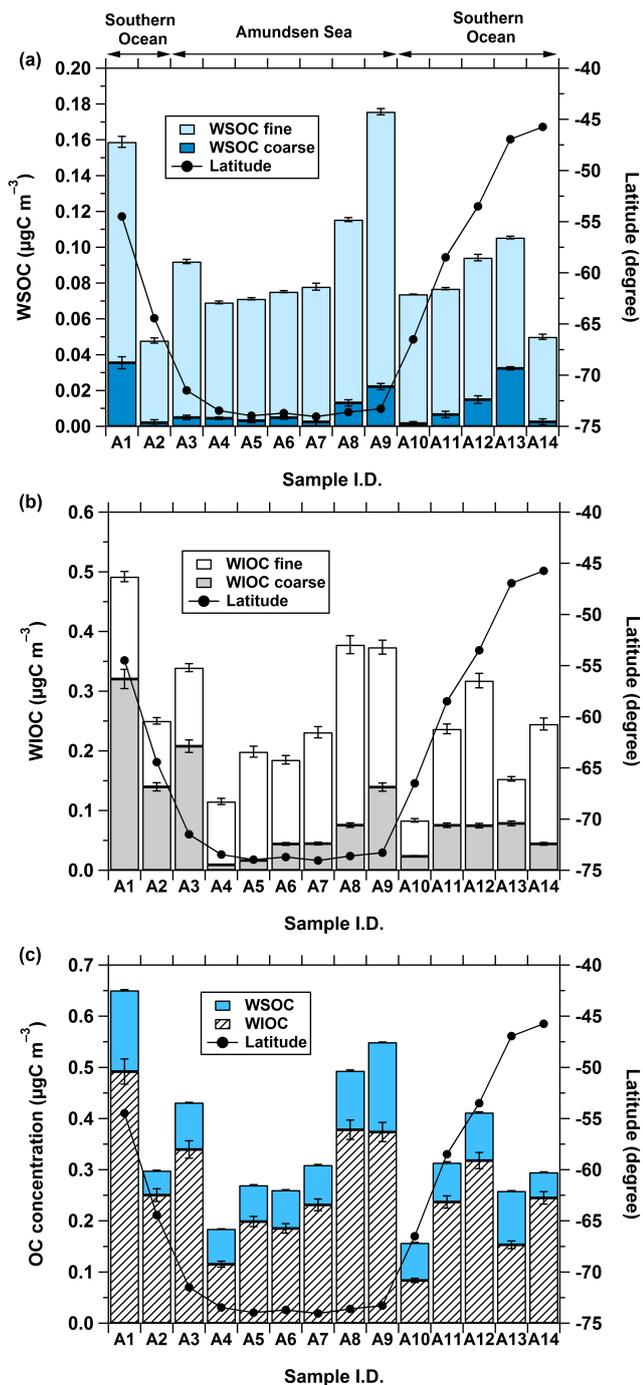
Figure 6. Concentrations of water-soluble organic carbon (WSOC) (a), water-insoluble organic carbon (WIOC) (b), and organic carbon (i.e., OC = WSOC + WIOC) (c) against sample I.D. in aerosols collected over the Southern Ocean (43°S−70°S) and the Amundsen Sea (70°S−75°S). Black solid circle lines indicate the latitude of half-way point between each aerosol sampling start and endpoint. Double arrows in panel (a) show the sampling locations of aerosol samples.
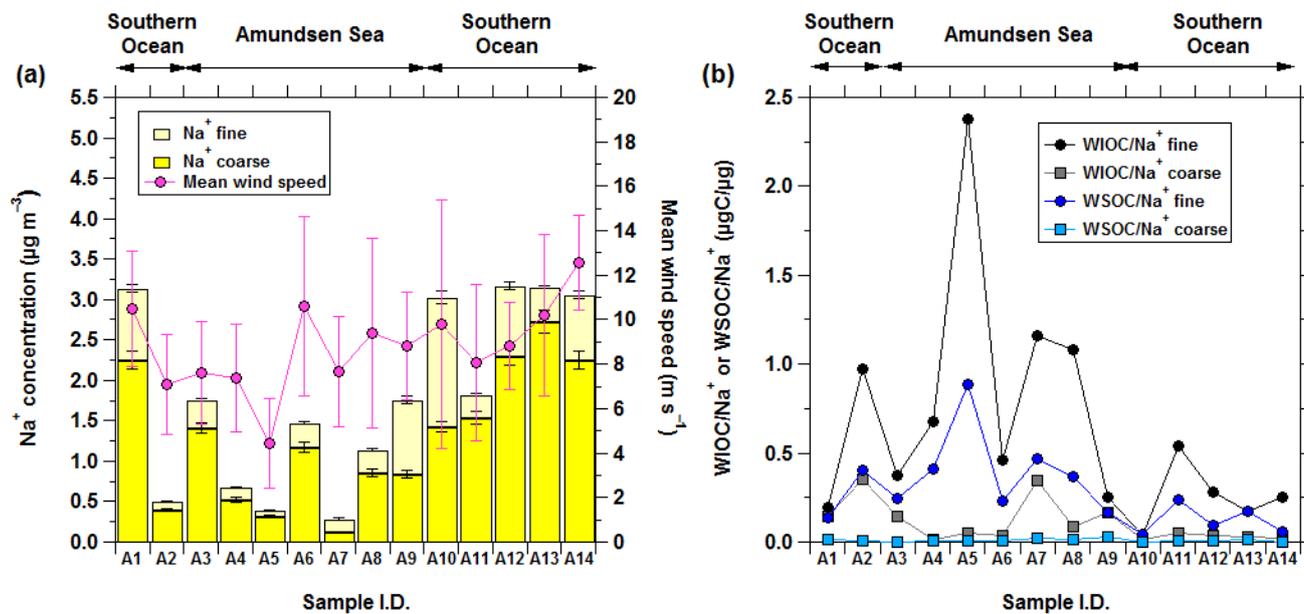
Figure 7. Concentration of Na⁺ (a), WIOC/Na⁺ and WSOC/Na⁺ ratios in both fine and coarse modes (b) against aerosol sample I.D. Pink solid circle line in panel (a) indicates the mean and standard deviation of wind speeds for each aerosol sampling time.
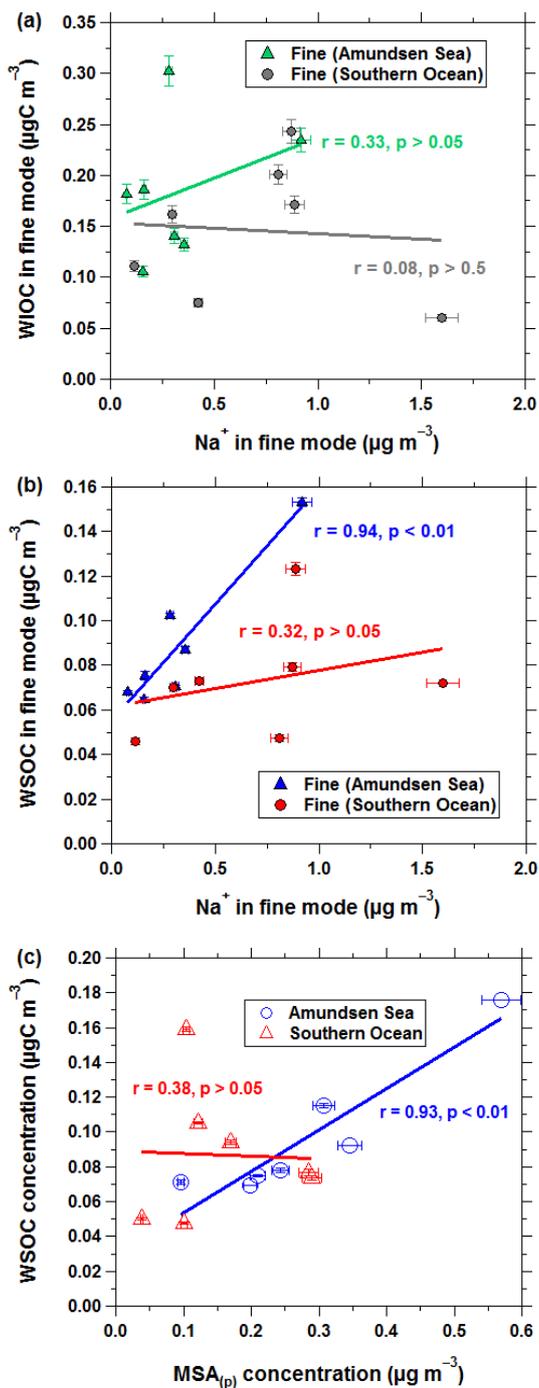
Figure 8. Relationships of WIOC (a) and WSOC (b) with Na⁺ in fine modes over the Southern Ocean (solid triangles) and the Amundsen Sea (solid circles). Panel (c) shows relationships between WSOC and MSA$_{(p)}$ concentrations over the Southern Ocean (open triangles) and the Amundsen Sea (open circles).
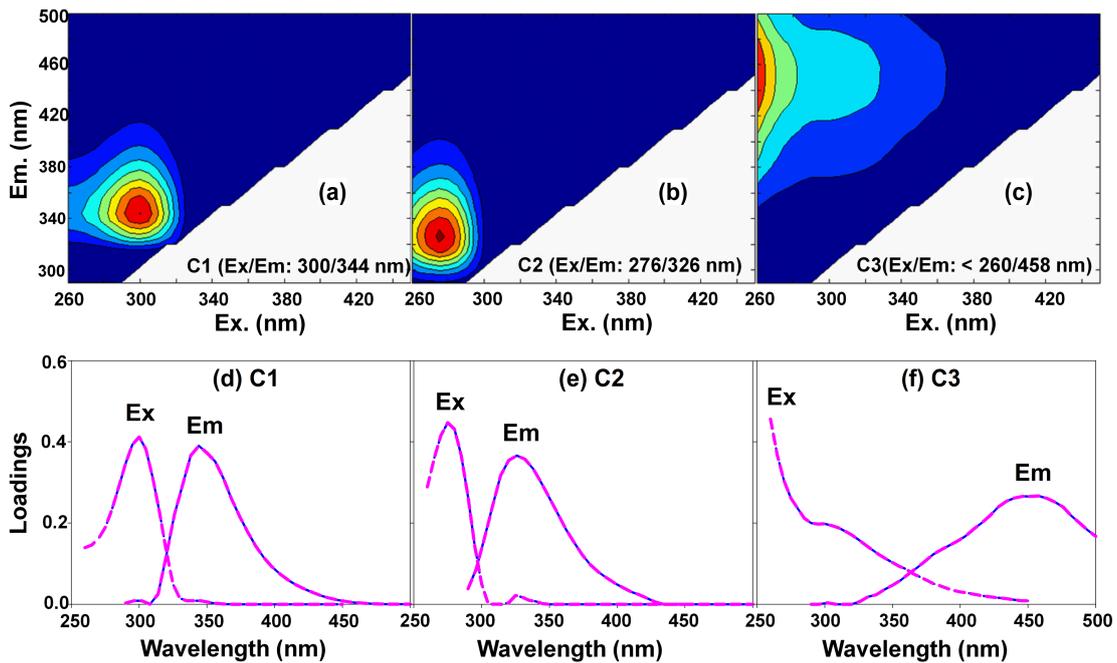
Figure 9. EEM contour plots of three fluorescent components C1−C3 (a−c) identified using EEM-PARAFAC in the fine mode aerosol particles (D < 2.5 µm) collected over the Southern Ocean and the Amundsen Sea, and excitation and emission spectra of C1−C3 (d−f).
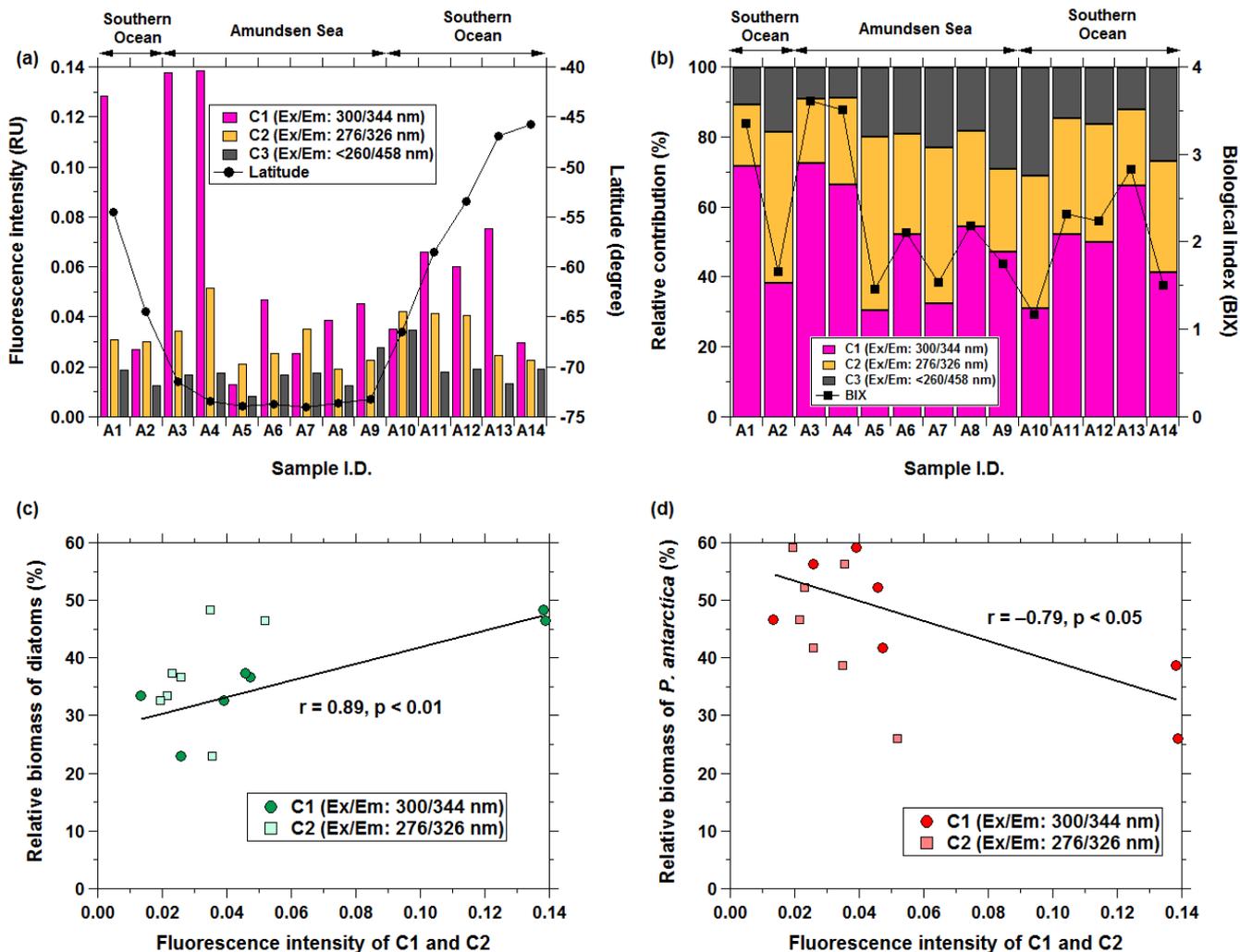
Figure 10. Variations of fluorescence intensities (a), relative contributions of C1−C3 and biological index (black solid square line) (b) in the fine mode aerosol particles (D < 2.5 μm) collected over the Southern Ocean and the Amundsen Sea. Black solid circle line in panel (a) indicates the latitude of half-way point between each aerosol sampling start and endpoint. Double arrows in panel (a) show the sampling locations of aerosol samples. Panels (c) and (d) show the relationship of fluorescence intensity of C1 with the relative biomass of diatoms and *Phaeocystis antarctica* (*P. antarctica*) observed in the Amundsen Sea, respectively.